TABLE 1. Cardiac catheterization data

	Hybrid therapy	Cardiac support device alone	ONO-1301 alone	Sham
dp/dt maximum (mm Hg/s)				
LV	1822 ± 83*,†,‡	1584 ± 114	1601 ± 91	1238 ± 127
RV	547 ± 101	450 ± 53	539 ± 79	443 ± 86
Ees (mm Hg/mL)				
LV	10 ± 1*,†,‡	7 ± 1	8 ± 1	4 ± 1
RV	3 ± 1	3 ± 1	3 ± 1	2 ± 1
−dp/dt minimum (mm Hg/s)				
LV	1553 ± 61*,†,‡	1303 ± 71	1387 ± 64	1061 ± 107
RV	407 ± 59	378 ± 67	412 ± 88	333 ± 78
Time constant of relaxation (s)				
LV	33 ± 4*,†	42 ± 3	36 ± 3	47 ± 5
RV	39 ± 6	40 ± 2	38 ± 4	46 ± 6

Data are mean ± standard deviation. *RV*, Right ventricular; *LV*, left ventricular. *$P < .05$ versus sham. †$P < .05$ versus cardiac support device alone. ‡$P < .05$ versus ONO-1301 alone.

further in the sham group, remained the same in the cardiac support device alone and ONO-1301 alone groups, and recovered in the hybrid therapy group (Figure 1, *E*).

In addition, systolic function represented by LV dp/dt max and Ees at 8 weeks was greater in the cardiac support device alone and ONO-1301 alone groups compared with the sham group, whereas the hybrid therapy showed significantly greater dp/dt max and Ees than the other groups (Table 1). LV -dp/dt min, which represents diastolic function, also was significantly greater in the hybrid therapy group at 8 weeks than in the other groups. LV time constant of relaxation, which is also an index of diastolic function, was significantly smaller in the hybrid therapy group at 8 weeks postinfarction than in the cardiac support device alone and sham groups. There were no significant differences in any of these parameters in the right ventricle.

MI induction also resulted in an increase in plasma NT-proBNP, assessed by an enzyme-linked immunosorbent assay kit (Cardiopet proBNP; IDEXX Laboratories, Tokyo, Japan), at 1 week postinfarction (Figure 1, *F*). NT-proBNP continued to increase in the sham group, whereas the increase was suppressed in each of the other groups after treatment. NT-proBNP decreased gradually in the hybrid therapy group and was significantly lower than in the sham group at 5 weeks, and was significantly lower than in the other 2 groups at 8 weeks.

Functional Recovery of Infarct Border Area With Hybrid Therapy

Regional LV wall motion was evaluated using speckle-tracking echocardiography to dissect region-specific functional effects of the treatment. The infarct area showed a significant and marked reduction in the radial strain after induction of MI, with no significant differences among the 4 groups (Table 2). Radial strain levels in the border area decreased similarly in all groups at 1 week postinfarction, although at 8 weeks the hybrid therapy group showed the greatest recovery in this area. There was a marked decrease in radial strain in the remote area in the sham group at 8 weeks, but there was little change throughout the study in the other groups.

Reduction in Global End-Systolic/Diastolic Wall Stress With Hybrid Therapy

Changes in global end-systolic/end-diastolic wall stresses after treatment were assessed from MDCT and catheterization data (Table 2). Similar increases in global end-systolic wall stress were observed in all groups at 1 week postinfarction. At 8 weeks postinfarction, however, there was a further increase in the sham group, a slight reduction in the cardiac support device alone group, and almost no change in the ONO-1301 alone group, whereas global end-systolic wall stress was lowest in the hybrid therapy group. Similar increases in global end-diastolic wall stress were observed in all groups at 1 week postinfarction. The sham group showed a marked increase at 8 weeks postinfarction, whereas the hybrid therapy and cardiac support device alone groups showed notable reductions. Global end-diastolic wall stress was significantly lower in the hybrid therapy group compared with the ONO-1301 alone and sham groups at 8 weeks.

ONO-1301 Induced Angiogenic Myocardial Effects in Chronic MI

The angiogenic effects of the treatment were evaluated by assessing global myocardial blood flow at rest by ^{13}N-ammonia PET at 8 weeks postinfarction. Myocardial blood flow in the hybrid therapy group was similar to that in the ONO-1301 group, and both were significantly higher than in the cardiac support device alone and sham groups (Figure 2). Capillary densities in the border and remote areas at 8 weeks postinfarction, which was measured by immunostaining for CD31, was significantly greater in the hybrid therapy group than in the cardiac support device alone and sham groups (Figure 3, *A*).

TABLE 2. Regional left ventricular wall motion and global left ventricular wall stress

	Hybrid therapy	Cardiac support device alone	ONO-1301 alone	Sham
Radial strain in the MI area (%)				
Pre-infarction	21.4 ± 2.3	20.9 ± 1.0	21.7 ± 2.4	22.4 ± 2.3
1 week post-infarction	7.1 ± 1.0	6.7 ± 0.7	7.5 ± 0.9	7.0 ± 1.0
8 weeks postinfarction	8.7 ± 1.2	7.3 ± 0.4	7.5 ± 1.3	6.7 ± 1.0
Radial strain in the border area (%)				
Pre-infarction	22.2 ± 2.6	21.8 ± 2.5	22.0 ± 1.6	21.3 ± 1.8
1 week postinfarction	10.4 ± 1.9	10.3 ± 1.9	11.2 ± 1.5	11.5 ± 1.9
8 weeks postinfarction	14.7 ± 1.1*,†,‡	10.8 ± 0.2	13.1 ± 1.7	8.1 ± 1.1
Radial strain in the remote area (%)				
Pre-infarction	20.7 ± 2.3	21.6 ± 2.0	21.0 ± 2.8	21.2 ± 2.7
1 week postinfarction	19.2 ± 2.1	20.5 ± 1.2	20.9 ± 2.2	19.6 ± 2.0
8 weeks postinfarction	20.2 ± 1.8*	19.7 ± 1.1	20.1 ± 1.5	14.8 ± 1.4
Global end-systolic wall stress (kdyne/cm^2)				
Pre-infarction	79.9 ± 6.8	84 ± 12.0	80.5 ± 8.1	87.6 ± 9.5
1 week postinfarction	108.1 ± 9.1	104.8 ± 11.9	102.7 ± 11.4	107.5 ± 9.6
8 weeks postinfarction	84 ± 5.7*,†,‡	97.7 ± 11.4	104.6 ± 10.0	161.9 ± 9.3
Global end-systolic wall stress (kdyne/cm^2)				
Pre-infarction	13.0 ± 1.5	11.5 ± 1.1	12.0 ± 1.3	12.0 ± 1.6
1 week postinfarction	17.9 ± 1.5	17.1 ± 1.0	17.0 ± 1.4	16.4 ± 2.5
8 weeks postinfarction	14.0 ± 2.5*,‡	14.0 ± 1.8	18.0 ± 1.5	24.4 ± 3.6

Data are mean ± standard deviation. *MI*, Myocardial infarction. *P < .05 versus sham. †P < .05 versus cardiac support device alone. ‡P < .05 versus ONO-1301 alone.

Histologic Evidence of Reversal of LV Remodeling With Hybrid Therapy

Pathologic cardiomyocyte hypertrophy and interstitial fibrosis in the border and remote areas at 8 weeks postinfarction were assessed by periodic acid-Schiff and Masson trichrome staining, respectively, to evaluate the degree of reversal of LV remodeling induced by each treatment (Figure 3, *B* and *C*). Cardiomyocyte diameters were significantly smaller in the border area in the hybrid therapy group compared with the ONO-1301 alone and sham groups, and were significantly smaller in the remote area compared with the sham group. In addition, there was significantly less interstitial fibrosis in the hybrid therapy group compared with the cardiac support device alone, ONO-1301 alone, and sham groups in the border area, and less than in the sham group in the remote area.

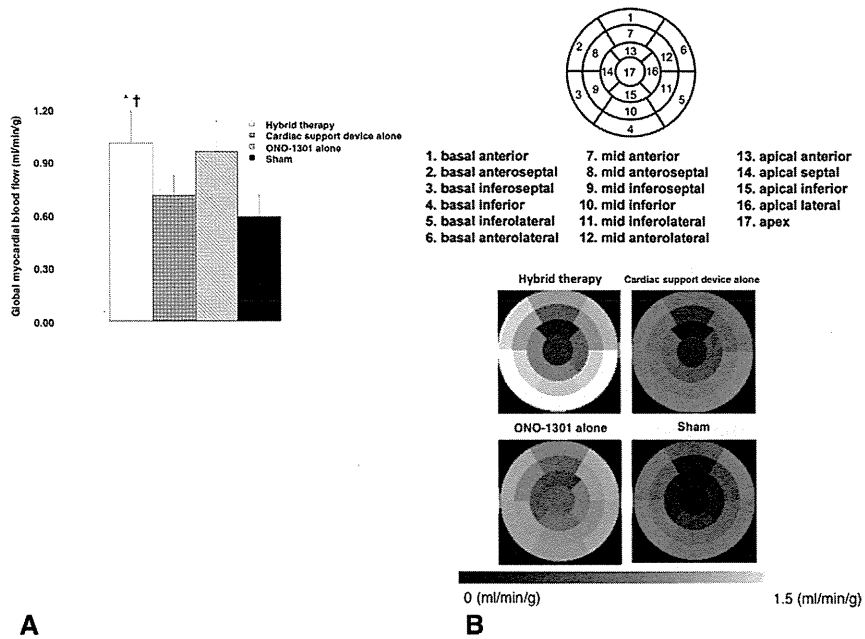

FIGURE 2. A, Global myocardial blood flow assessed by PET at 8 weeks postinfarction. B, Myocardial blood flow divided into 17 segments recommended by the American Heart Association. *P < .05 versus sham, †P < .05 versus cardiac support device alone.

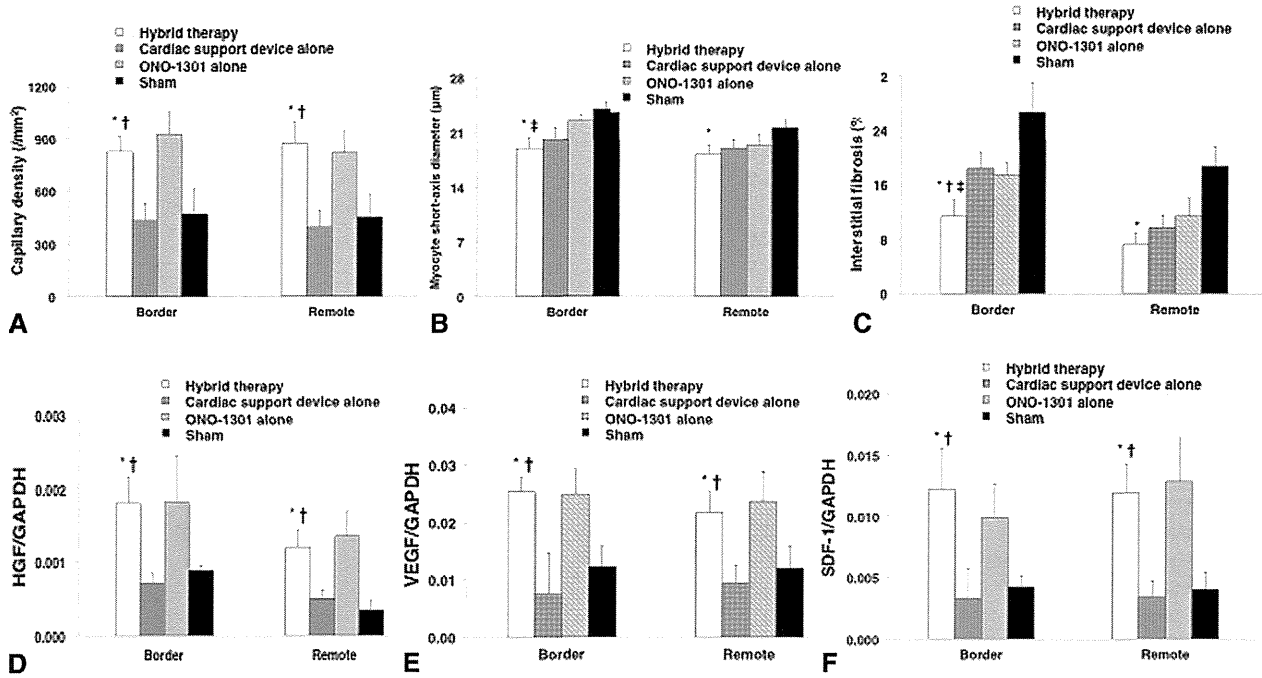

FIGURE 3. Histologic evaluation at 8 weeks postinfarction. A, Capillary density, (B) myocyte short-axis diameter, and (C) interstitial fibrosis in the border and remote areas. Expression levels of (D) HGF, (E) VEGF, and (F) SDF-1 in the border and remote areas quantified by real-time polymerase chain reaction at 8 weeks postinfarction. *$P < .05$ versus sham, †$P < .05$ versus cardiac support device alone. *GAPDH*, Glyceraldehyde 3-phosphate dehydrogenase; *HGF*, hepatocyte growth factor; *VEGF*, vascular endothelial growth factor; *SDF-1*; stromal cell–derived factor-1.

Up-Regulation of Cardiac Protective Factors

Real-time polymerase chain reaction was performed at 8 weeks postinfarction to determine the effects of the treatment on gene expression of major cardiac protective factors, such as HGF, VEGF and SDF-1 (Figure 3, *D-F*). Expression of HGF, VEGF, and SDF-1 in both the border and remote areas were similar in the hybrid therapy and ONO-1301 groups, and significantly higher in these 2 groups than in the cardiac support device alone and sham groups ($P < .05$).

DISCUSSION

This study examined the therapeutic efficacy of hybrid therapy, comprising a cardiac support device and a synthetic prostacyclin agonist (ONO-1301), in a canine model of ischemic cardiomyopathy, compared with the efficacy of either treatment alone. Hybrid therapy significantly improved both systolic and diastolic functions and reduced LV wall stress compared with the other treatments, and histologic examination indicated significantly greater reversal of LV remodeling in the hybrid therapy group. These results were reflected by a significantly greater reduction of NT-proBNP by hybrid therapy.

The cardiac support device used in this study comprised a net made of polyglycolic acid, which is a hydrolytically bioabsorbable polymer. This represents a major difference from the net used in previous studies,[3-5] and was designed to remain around the heart for approximately 10 weeks by adjusting the diameter of the thread. The cardiac support device remained in place at 8 weeks postinfarction, although it had become hydrolyzed to some extent. Our net was functionally equivalent to the nets used in previous studies; it prevented dilatation of the left ventricle, improved the LV sphericity index, and reduced diastolic LV wall stress, thus avoiding the positive feedback loop of cardiac dilatation, the change from an efficient ellipsoidal to a spherical LV chamber, interstitial fibrosis, and, ultimately, heart failure that occurs in ischemic dilated cardiomyopathy.[9] However, one disadvantage of this bioabsorbable net is that it could allow LV remodeling to progress after absorption. The present study did not investigate this aspect and further studies are needed to assess the relative advantages and disadvantages of bioabsorbable and nonabsorbable cardiac support devices.

ONO-1301 is a synthetic prostacyclin agonist that is not yet used in clinical practice. However, several experimental studies have shown its therapeutic efficacy in ischemic and nonischemic cardiomyopathy.[10-12] ONO-1301 was administered to the heart differently in the current study compared with previous studies,[10-12] but its plasma concentrations and reversal of LV remodeling were similar to those seen in previous studies, suggesting that this mode of administration was appropriate. In addition, ONO-1301 administration by incorporation in the cardiac support device could decrease

adverse effects such as hypotension, which may occur with systemic administration. Finally, LV remodeling generally progresses slowly, and long-term drug efficacy therefore is necessary. ONO-1301 has a slow-release time of approximately 4 weeks, and thus may be a suitable agent for the prevention of remodeling.

The favorable results of the current study regarding use of hybrid therapy may be attributed to the angiogenic and active antifibrotic effects of ONO-1301, acting via HGF, VEGF, and SDF-1, which complemented the mechanical effects of the cardiac support device with a consequent enhancement of therapeutic efficacy. Up-regulation of these cytokines and increased capillary density were observed in the hybrid therapy group, whereas PET examination showed significantly greater myocardial blood flow in the hybrid therapy group compared with the cardiac support device alone and sham groups. The additional benefits of ONO-1301 resulted in enhanced recovery of radial wall strain and the suppression of interstitial fibrosis in the border area in the hybrid therapy group, with consequent recovery of cardiac function.

This study was limited by the use of a canine model, which may not completely reflect clinical ischemic cardiomyopathy pathologies. In this experiment, there was no atherosclerosis, and no use of drugs such as β-blockers and angiotensin-converting enzyme inhibitors, which might be used in the clinical arena. However, a similar canine ischemic cardiomyopathy model has been established previously,[2,12] and it is possible to use this model to assess cardiac function and evaluate the therapeutic effects of interventions. Our model therefore was deemed adequate to show the therapeutic effects of the hybrid therapy with various modalities used in the clinical arena. However, this model may not be suitable for further studies of the mechanisms of hybrid therapy, and rodent models may be better suited for such investigations. This study also was limited in that it was not clear whether remodeling would remain suppressed even after complete absorption of the cardiac support net because the net remained at the end of this study. Therefore, longer-term studies lasting after absorption of the biodegradable net will be necessary.

The authors thank Shigeru Matsumi, Toshika Senba, Masako Yokoyama, and Akima Harada for excellent technical assistance.

References

1. Pfeffer MA, Braunwald E. Ventricular remodeling after myocardial infarction: experimental observations and clinical implications. *Circulation.* 1990;81: 1161-72.
2. Moreira LF, Stolf NA, de Lourdes Higuchi M, Bacal F, Bocchi EA, Oliveira SA. Current perspectives of partial left ventriculectomy in the treatment of dilated cardiomyopathy. *Eur J Cardiothorac Surg.* 2001;19:54-60.
3. Chaudhry PA, Mishima T, Sharov VG, Hawkins J, Alferness C, Paone G, et al. Passive epicardial containment prevents ventricular remodeling in heart failure. *Ann Thorac Surg.* 2000;70:1275-80.
4. Chaudhry PA, Anagnostopouls PV, Mishima T, Suzuki G, Nair H, Morita H, et al. Acute ventricular reduction with the acorn cardiac support device: effect on progressive left ventricular dysfunction and dilation in dogs with chronic heart failure. *J Cardiac Surg.* 2001;16:118-26.
5. Pilla JJ, Blom AS, Brockman DJ, Bowen F, Yuan Q, Giammarco J, et al. Ventricular constraint using the acorn cardiac support device reduces myocardial akinetic area in an ovine model of acute infarction. *Circulation.* 2002;106:I207-11.
6. Lembcke A, Dusche S, Enzweiller CN, Kloeters C, Wiese TH, Hermann KG, et al. Passive external cardiac constraint improves segmental left ventricular wall motion and reduces akinetic area in patients with non-ischemic dilated cardiomyopathy. *Eur J Cardiothorac Surg.* 2004;25:84-90.
7. Mann DL, Acker MA, Jessup M, Sabbah HN, Starling RC, Kubo SH, Acorn Trial Principal Investigators and Study Coordinators. Clinical evaluation of the CorCap Cardiac Support Device in patients with dilated cardiomyopathy. *Ann Thorac Surg.* 2007;84:1226-35.
8. Mann DL, Kubo SH, Sabbah HN, Starling RC, Jessup M, Oh JK, et al. Beneficial effects of the CorCap cardiac support device: five-year results from the Acorn Trial. *J Thorac Cardiovasc Surg.* 2012;143:1036-42.
9. Atluri P, Acker MA. Diastolic ventricular support with cardiac support devices: an alternative approach to prevent adverse ventricular remodeling. *Heart Fail Rev.* 2013;18:55-63.
10. Nakamura K, Sata M, Iwata H, Sakai Y, Hirata Y, Kugiyama K, et al. A synthetic small molecule, ONO-1301, enhances endogenous growth factor expression and augments angiogenesis in the ischaemic heart. *Clin Sci (Lond).* 2007;112:607-16.
11. Iwata H, Nakamura K, Sumi M, Ninomiya M, Sakai Y, Hirata Y, et al. Local delivery of synthetic prostacycline agonist augments collateral growth and improves cardiac function in a swine chronic cardiac ischemia model. *Life Sci.* 2009;85:255-61.
12. Shirasaka T, Miyagawa S, Fukushima S, Saito A, Shiozaki M, Kawaguchi N, et al. A slow-releasing form of prostacycline agonist (ONO1301SR) enhances endogenous secretion of multiple cardiotherapeutic cytokines and improves cardiac function in rapid-pacing induced canine heart failure model. *J Thorac Cardiovasc Surg.* 2013;146:413-21.
13. Kawamura M, Miyagawa S, Miki K, Saito A, Fukushima S, Higuchi T, et al. Feasibility, safety, and therapeutic efficacy of human induced pluripotent stem cell-derived cardiomyocyte sheets in a porcine ischemic cardiomyopathy model. *Circulation.* 2012;126(Suppl 1):S29-37.
14. Takeda K, Taniguchi K, Shudo Y, Kainuma S, Hamada S, Matsue H, et al. Mechanism of beneficial effects of restrictive mitral annuloplasty in patients with dilated cardiomyopathy and functional mitral regurgitation. *Circulation.* 2010; 122(Suppl):S3-9.

Synthetic prostacyclin agonist, ONO1301, enhances endogenous myocardial repair in a hamster model of dilated cardiomyopathy: A promising regenerative therapy for the failing heart

Kazuhiko Ishimaru, MD, Shigeru Miyagawa, MD, PhD, Satsuki Fukushima, MD, PhD, Atsuhiro Saito, PhD, Yoshiki Sakai, PhD, Takayoshi Ueno, MD, PhD, and Yoshiki Sawa, MD, PhD

Objectives: Remodeling of the left ventricle (LV) in idiopathic dilated cardiomyopathy (IDCM) is known to be associated with multiple pathologic changes that endogenous factors, such as hepatocyte growth factor (HGF) and vascular endothelial growth factor (VEGF), protect against. Although a clinically relevant delivery method of these factors has not been established, ONO1301, a synthetic prostacyclin agonist, has been shown to upregulate multiple cardioprotective factors, including HGF and VEGF, in vivo. We thus hypothesized that ONO1301 may reverse LV remodeling in the DCM heart.

Methods: ONO1301 dose-dependently added to the normal human dermal fibroblasts and human coronary artery smooth muscle cells in vitro, to measure the expression of HGF, VEGF, stromal cell–derived factor (SDF)-1, and granulocyte-colony stimulating factor (G-CSF), assessed by real-time polymerase chain reaction (PCR) and enzyme-linked immunosorbent assay. δ-Sarcoglycan-deficient J2N-k hamsters, which is an established DCM model, were treated by epicardial implantation of an atelocollagen sheet with or without ONO1301 immersion or sham operation.

Results: ONO1301 dose-dependently upregulated expression of these 4 factors in vitro. ONO1301 treatment, which induced dominant elevation of ONO1301 levels for 2 weeks, significantly preserved cardiac performance and prolonged survival compared with the other groups. This treatment significantly upregulated expressions of cardioprotective factors and was associated with increased capillaries, attenuated fibrosis, and upregulation of α-sarcoglycan in the DCM heart.

Conclusions: ONO1301 atelocollagen-sheet implantation reorganized cytoskeletal proteins, such as α-sarcoglycan, increased capillaries, reduced fibrosis, and was associated with upregulated expression of multiple cardioprotective factors, leading to preservation of cardiac performance and prolongation of survival in the δ-sarcoglycan-deficient DCM hamster. (J Thorac Cardiovasc Surg 2013;146:1516-25)

Idiopathic dilated cardiomyopathy (IDCM) is one of the most critical intractable diseases. The etiology and pathology of IDCM have therefore been intensively investigated to explore other treatment options.[1] Clinical and functional progression of IDCM has been shown to be closely correlated with the histopathology, such as apoptosis of cardiomyocytes, accumulation of fibrotic components, reduction of vascular density, and remodeling of sarcolemmal/cytoskeletal proteins. It has been recently suggested that cell transplantation into the IDCM heart positively modulates cellular behavior of native cardiac fibroblasts and/or coronary artery smooth muscle cells (CoASMCs), leading to upregulation of multiple cardioprotective factors in the heart.[2] Inasmuch as cell transplantation is clinically limited by the cell-culture procedure and the availability of a cell processing center, cell-free therapy that enhances cardiac regeneration has long been sought in the clinical arena.[3]

Prostacyclin and its analogs have been shown to upregulate expressions of various factors, such as hepatic growth factor (HGF) and vascular endothelial growth factor (VEGF) in vitro and in vivo.[4] Although previously generated prostacyclin agonists are chemically unstable, being limited by the delivery method, it has recently been shown that ONO1301 is a selective prostacyclin receptor (IPR) agonist having a unique, chemically stable structure, and polymerization of ONO1301 with polylactic-co-glycolic acid copolymer (PLGA) to form a microsphere (ONO1301-MS) upregulates multiple protective factors, represented by HGF, for 3 to 4 weeks in vivo.[5] We therefore

From the Department of Cardiovascular Surgery, Osaka University Graduate School of Medicine, Osaka, Japan.

This study was financially supported by Grants for the Research and Development of the Myocardial Regeneration Medicine Program from the New Energy Industrial Technology Development Organization (NEDO), Japan.

Disclosures: Yoshiki Sakai is the holder of the patent for ONO1301 encapsulated with PLGA microspheres; All other authors have nothing to disclose with regard to commercial support.

Received for publication Nov 14, 2012; revisions received Feb 8, 2013; accepted for publication Feb 14, 2013.

Address for reprints: Yoshiki Sawa, MD, PhD, Department of Cardiovascular Surgery, Osaka University Graduate School of Medicine, 2-2 Yamadaoka, Suita 565-0871, Japan (E-mail: sawa-p@surg1.med.osaka-u.ac.jp).

0022-5223/$36.00

http://dx.doi.org/10.1016/j.jtcvs.2013.02.045

Abbreviations and Acronyms

CoASMC = coronary artery smooth muscle cell
DCM = dilated cardiomyopathy
Dd/Ds = diastolic/systolic dimensions
EF = ejection fraction
ELISA = enzyme-linked immunosorbent assay
GAPDH = glyceraldehyde-3-phosphate dehydrogenase
G-CSF = granulocyte colony stimulating factor
HCoASMC = human coronary artery smooth muscle cell
HGF = hepatic growth factor
IPR = prostacyclin receptor
IDCM = idiopathic dilated cardiomyopathy
LV = left ventricular (ventricle)
N group = atelocollagen sheet without ONO1301
NHDF = normal human dermal fibroblast
O group = atelocollagen sheet containing ONO1301
PCR = polymerase chain reaction
PLGA = polylactic-co-glycolic acid copolymer
S group = sham group
SDF-1 = stromal cell–derived factor-1
VEGF = vascular endothelial growth factor
vWF = von Willebrand factor

hypothesized that administration of ONO1301-MS into the IDCM heart might upregulate cardiac protective factors, leading to histologic and functional reverse left ventricular (LV) remodeling.

MATERIALS AND METHODS

Experimental procedures related to animal studies were carried out under the approval of the institutional ethics committee. The investigation conformed to the "Principles of Laboratory Animal Care" formulated by the National Society for Medical Research and the "Guide for the Care and Use of Laboratory Animals" (National Institutes of Health Publication No. 85 to 23, revised 1996). All experimental procedures and evaluations were performed in a blinded manner.

Cell Culture

Normal human dermal fibroblasts (NHDFs) and human CoASMCs (HCoASMCs) were purchased from EIDIA Co, Ltd (Tokyo, Japan). The cells were cultured on 6-well plates with Dulbecco's modified Eagle's medium (Sigma-Aldrich, St Louis, Mo) supplemented with 10% fetal bovine serum (EIDIA) under 5% carbon dioxide. Next, 1- to 1000-nmol/L ONO1301 (Ono Pharmaceutical, Osaka, Japan), dimethyl sulphoxide (Sigma-Aldrich) or dibutyryl cyclic adenosine monophosphate (Sigma-Aldrich) was added to the culture medium for 72 hours, and then the culture supernatants and cells (n = 6, respectively) were harvested and stored at −80°C.

Procedure of ONO1301-MS Administration to the Dilated Cardiomyopathy (DCM) Hamster

Male 20-week-old δ-sarcoglycan-deficient J2N-k hamsters and J2N-n normal hamsters were purchased from Japan SLC (Shizuoka, Japan). Inasmuch as human DCM-like histopathologic features and associated functional deterioration develop in J2N-k hamsters, they have been used as an established IDCM model.[6] Each hamster underwent left lateral thoracotomy under 1.5% isoflurane anesthesia (n = 66). Subsequently, ONO-1301 was delivered into the heart using a novel drug delivery system, in which an atelocollagen sheet (Integran sheet; Koken Co, Ltd, Tokyo, Japan) shaped "hand-drum" containing ONO1301-MS (10 mg/kg) was placed to cover the entire ventricular free wall (O group, n = 22). Other hamsters underwent either ONO1301-free atelocollagen sheet implantation in the same manner (N group, n = 21) or sham operation (S group, n = 23). After the layered closure, the hamsters were housed in a temperature-controlled individual cage until spontaneous or scheduled death at 2 or 4 weeks after the operation (n = 5 each).

Measurement of ONO1301 Concentration in the Plasma and the Ventricular Tissue

Under isoflurane inhalation (5%), venous blood (1 mL) was sampled from the internal jugular vein, and the ventricle was then excised from the hamster at day 1 and weeks 1, 2, 4, and 8 after ONO1301 treatment (n = 3 each). The plasma was stored at −80°C, and the ventricle was thoroughly washed and stored at −80°C. The concentrations of ONO1301 in the plasma and the ventricle were measured by high-performance liquid chromatography with the tandem mass spectrometric (LC/MS/MS) detection.[7]

Transthoracic Echocardiography

Transthoracic echocardiography was performed using a system equipped with a 12-MHz transducer and SONOS 5500 (Agilent Technologies, Palo Alto, Calif) under isoflurane inhalation (1%). Diastolic/systolic dimensions (Dd/Ds) and ejection fraction (EF) of the LV were measured.[8]

Histopathology

The heart was excised under isoflurane anesthesia (5%) and immersion-fixed with ice cold 4% paraformaldehyde. The fixed heart was embedded with either paraffin or optimal cutting temperature compound (Funakoshi, Tokyo, Japan) and transversely sliced to generate paraffin or frozen sections, respectively. The paraffin sections were stained using picrosirius red or immunohistologically labeled using anti–von Willebrand factor (vWF) antibody (DAKO, Glostrup, Denmark). Frozen sections (7-μm thick) were immunohistologically labeled using anti–α-dystroglycan (clone: VIA4-1; Upstate Biotechnology, Lake Placid, NY), anti–α-sarcoglycan (clone: Ad1/20A6; Novocastra, Wetzlar, Germany), anti–β-sarcoglycan (clone: bSarc/5B1; Novocastra), anti-IPR (Abcam, Cambridge, United Kingdom), or anti–α-actin (Millipore, Billerica, Mass) antibodies. The sections were then labeled by corresponding AlexaFluor488/594-conjugated secondary antibodies counterstained with 6-diamidino-2-phenylindole (DAPI; Life Technologies, Calif). 3,3′-Diaminobenzidine (DAB) staining of IPR was performed using the LSAB2 kit (DAKO). Fluorescent-labeled sections were viewed under an ECLIPSE TE 200-U confocal microscope (Nikon, Tokyo, Japan). The percentage of the total area that was fibrotic, as determined by picrosirius red staining, was calculated by using a planimetric method with MetaMorph software (Molecular Device, Osaka, Japan). The number of capillaries per square millimeter was calculated by the BZ Analyzer (Keyence, Osaka, Japan) and was counted in 4 high-power fields per section (a total of 10-12 fields/heart).

Real-Time Polymerase Chain Reaction

Total RNA was isolated from the cultured cells and the free wall of the LV using the RNeasy Kit and reverse-transcribed using Omniscript Reverse

TABLE 1. Forward and reverse primers and probe

	F-primer	R-primer	Probe
Human			
GAPDH	GAA GGT GAA GGT CGG AGT C	GAA GAT GGT GAT GGG ATT TC	CAA GCT TCC CGT TCT CAG CC
HGF	ATG ATG TCC ACG GAA GAG GAG A	CAC TCG TAA TAG GCC ATC ATA GTT GA	TGC AAA CAG GTT CTC AAT GTT TCC CAG C
VEGF	GAA GTG GTG AAG TTC ATG GAT GTC T	CAC ACA GGA TGG CTT GAA GAT G	TTC CAG GAG TAC CCT GAT GAG ATC GA
SDF-1	CAT GCC GAT TCT TCG AAA GC	CTA CAA TCT GAA GGG CAC AGT TTG	TGT TGC CAG AGC CAA CGT CAA GCA
G-CSF	GCT GTG GCA CAG TGC ACT CT	CCC TGG ATC TTC CTC ACT TGC TC	CCT GCC CCA GAG CTT CCT GCT CA
Hamster			
GAPDH	CTG CAC CAC CAC CTG CTT AGC	GCC ATG CCA GTG AGC TTC C	CTG CAC CAC CAC CTG CTT AGC
HGF	AGG TCC CAT GGA TCA CAC AGA	GCC CTT GTC GGG ATA TCT TTC T	ACC AGC AGA CAC CAC ACC GGC A
VEGF	GCA CTG GAC CCT GGC TTT ACT	TCA TGG GAC TTC TGC TCT CCT T	ACC ATG CCA AGT GGT CCC AGG CT
α-Sarcoglycan	AAC TGA AGA GAG ACA TGG CCA CC	CAG TGC TGG TCC AGG ATG AGG	CCT CTC TCC ACC TTG CCC ATG TTC A
β-Sarcoglycan	TCC ACT GAG AGG ATT ACC AGC AAT	AGT TTG TAG CGC ACC CAG TCA C	TCC TCA ATG GAA CTG TGA TGG TCA GCC C
α-Dystroglycan	CAC ACA GTC ATT CCA GCT GTT GT	TCA TCC AGC TCG TCT GCA AAG	CCT TGA GGA CCA GGC CAC CTT TAT CAA

GAPDH, Glyceraldehyde-3-phosphate dehydrogenase; *HGF*, hepatic growth factor; *VEGF*, vascular endothelial growth factor; *SDF-1*, stromal cell–derived factor-1; *G-CSF*, granulocyte colony stimulating factor.

transcriptase (Qiagen, Hilden, Germany). Quantitative polymerase chain reaction (PCR) was performed with the ABI 7500 Fast Real-Time PCR using TaqMan Universal Master Mix (Applied Biosystems, Division of Life Technologies Corporation, Carlsbad, Calif) and the designed primers/probes (Table 1). Expression of each mRNA was normalized to that of glyceraldehyde-3-phosphate dehydrogenase (GAPDH).

Western Blotting

The LV free wall was homogenized and centrifuged at 1000 g at 4°C for 10 minutes to retrieve protein. Subsequently, 10 to 20 μg of protein was subjected to sodium dodecyl sulfate polyacrylamide gel electrophoresis with 12.5% gels and transferred to polyvinylidene difluoride membranes (GE Healthcare, Little Chalfont, United Kingdom) using the Mini Trans-Blot system (170-3930; Bio-Rad Laboratories, Hercules, Calif). Protein blots in polyvinylidene difluoride membranes were incubated with each of the primary antibodies against α-sarcoglycan or GAPDH (Abcam, Plc, Cambridge, United Kingdom). The membranes were incubated with the corresponding horseradish peroxidase–labeled secondary antibody and then visualized using the ECL system (GE Healthcare Lifesciences, Cleveland, Ohio). The band intensities were quantified by Image-J software (Wine Rasband, Bethesda, Md). The values obtained were expressed as a percentage of the value in the J2N-n hamsters.

Statistical Analysis

Data are summarized as means ± SEMs. Comparisons among groups were made with the use of 1-way analysis of variance, followed by the Tukey honestly significant difference test. Differences across the whole time course of echocardiographic data and the concentration of ONO1301 were analyzed by repeated analysis of variance including main effects of the group, time, and their interactive effects, followed by pairwise comparisons at different times using a paired *t* test with the Bonferroni multiplicity correction. Survival curves were prepared by using the Kaplan-Meier method and compared using the log-rank test. All probability values are 2-sided. Statistical analysis was performed by using SPSS version 11.0 (SPSS, Inc, Chicago, Ill).

RESULTS

Effects of ONO1301 on the Secretion of Protective Factors in Vitro

Dose-dependent effects of ONO1301 on each component of the cells were assessed by cultivating commercially available NHDFs, HCoASMCs in vitro. Synthesis and extracellular secretion of protective factors were quantitatively assessed by real-time PCR and enzyme-linked immunosorbent assay (ELISA; Quantikine; R&D Systems, Minneapolis, Minn), respectively. ONO1301 treatment upregulated the expressions of HGF, VEGF, and stromal cell–derived factor-1 (SDF-1), but not granulocyte colony stimulating factor (G-CSF), in the NHDFs assessed by real-time PCR (Figure 1, *A*). In particular, a high concentration of ONO1301 significantly upregulated expressions of these factors. These findings were consistent with the results of ELISA for the culture supernatants (Figure 1, *B*). A high concentration of ONO1301 also significantly upregulated expressions of HGF, VEGF, and G-CSF, but not SDF-1, in the HCoASMCs, assessed by real-time PCR and ELISA (Figure 1, *C* and *D*).

Heart-Dominant Elevation of ONO1301 Concentration After ONO1301 Treatment

The difference in the ONO1301 concentration between the plasma and the LV after ONO1301 treatment was quantitatively and serially assessed by the LC/MS/MS method. The ventricular ONO1301 concentration was markedly greater than the plasma concentration at week 1 and week 2 after the treatment, although the plasma ONO1301 concentration

was higher than the detectable limit for this period (Figure 2, *A*). Both ventricular and plasma concentrations of ONO1301 were less than the detectable limit at weeks 4 and 8.

Presence of IPR in the Vasculature of the IDCM Heart

Localization of the IPR in the heart was assessed by immunohistolabeling. IPR was present in the microvasculature component, such as vascular SMCs and endothelial cells (Figure 2, *B* and *C*), but not in the cardiac fibroblasts or cardiomyocytes (Figure 2, *D*). Expression of the IPR was not different between the J2N-k and J2N-n hamsters.

Preserved Cardiac Performance in the IDCM Hamster With ONO1301 Therapy

The functional effects of ONO1301-atelocollagen sheet implantation on the IDCM heart were serially assessed by transthoracic echocardiography. LVDd/Ds and EF at 20 weeks of age, just before the treatment, were not significantly different among the 3 groups (Figure 2, *E*). After treatment, echocardiography showed that the LVDd/Ds and EF were significantly preserved until 4 weeks in the O group, compared with the N and S groups, which showed a progressive increase of LVDd/Ds and a progressive reduction of LVEF for the subsequent 8 weeks. However, even the O group showed progressively increased LVDd/Ds and reduced LVEF in the subsequent 4 weeks.

Upregulated HGF and VEGF in the Heart After ONO1301 Treatment

Real-time PCR was used to quantitatively assess the trend in expression of angiogenic factors, such as HGF and VEGF, in the hearts of the 3 groups and the normal hamster (n = 5, each). Intramyocardial mRNA levels of HGF and VEGF in the S and the N groups were not significantly different from those in the normal hamster at 2 or 4 weeks (Figure 3, *A*). In contrast, in the O group, both HGF and VEGF were significantly upregulated at 2 weeks compared with the other groups. VEGF significantly upregulated in the O group at 4 weeks, although the HGF level in the O group was not significantly different from that in the other groups at 4 weeks.

Increased Vasculature in the Heart After ONO1301 Treatment

The trend in the distribution and the number of arterioles and capillaries in the heart after ONO1301 treatment was assessed by vWF-labeled sections of the 3 groups and normal hamsters (n = 5, each). The number of vWF-positive arterioles and capillaries was significantly less in the N and the S groups than in the normal heart at 2 and 4 weeks. In contrast, vWF-positive arterioles and capillaries were homogeneously increased in the O group at 2 and 4 weeks compared with the other groups (Figure 3, *B*; $P < .05$).

Effect of ONO1301 on Myocardial Fibrosis

The distribution and the quantity of interstitial collagen in the heart after ONO1301 treatment was assessed by picrosirius red–stained sections (n = 5, each). Interstitial collagen was significantly accumulated in the J2N-k hamsters, regardless of the treatment, compared with the normal hamsters (Figure 3, *C*). However, collagen accumulation was significantly less in the O group than in the S and the N groups at 2 and 4 weeks.

Reorganization of Cytoskeletal Proteins After ONO1301 Treatment

The trend in the expression of α-sarcoglycan in the hearts after ONO1301 treatment was comprehensively assessed by immunohistolabeling, real-time PCR, and Western blotting analysis (Figure 4, *A-C*). α-Sarcoglycan was homogeneously expressed around the cardiomyocytes of the normal hamster, but it was rarely expressed in the heart of the N or S groups on immunoconfocal microscopy. In contrast, α-sarcoglycan expression was greater in the O group than in the N and S groups at 2 weeks, but not at 4 weeks. The mRNA of α-sarcoglycan was significantly greater in the O group than in the S and the N groups at 2 weeks, but not at 4 weeks. Consistently, Western blotting analysis in the heart showed significantly upregulated α-sarcoglycan expression at 2 weeks, but not at 4 weeks in the O group, compared with the S and the N groups. In addition, the trends in expressions of other cytoskeletal proteins, such as β-sarcoglycan and α-dystroglycan, after the ONO1301 treatment were assessed by immunohistolabeling and real-time PCR (Figure 4, *D* and *E*). β-Sarcoglycan was rarely expressed in the J2N-k hamster heart regardless of treatment, whereas expression of α-dystroglycan appeared to be greater in the O group than in the S and the N groups, although there were no significant differences.

Survival Benefit of ONO1301 Treatment in IDCM

No mortality or morbidity related to surgical procedure was identified in any of the groups. Survival of J2N-k hamsters after treatment was then assessed using the Kaplan-Meier method. Hamsters of the N and the S groups showed similar progression to death, primarily owing to congestive cardiac failure over the 4 weeks after treatment. In contrast, survival of hamsters in the O group was significantly prolonged compared with that of the other groups (Figure 5).

DISCUSSION

Summary of the Findings

In the present study, ONO1301 induced secretion of multiple cardiac protective factors such as HGF, VEGF, SDF-1, and G-CSF from NHDFs and HCoASMCs in a dose-dependent manner in vitro. Epicardial implantation of an ONO1301-immersed atelocollagen sheet, which was developed as a slow-releasing drug delivery system, induced heart-dominant elevation of ONO1301 for 2 weeks in

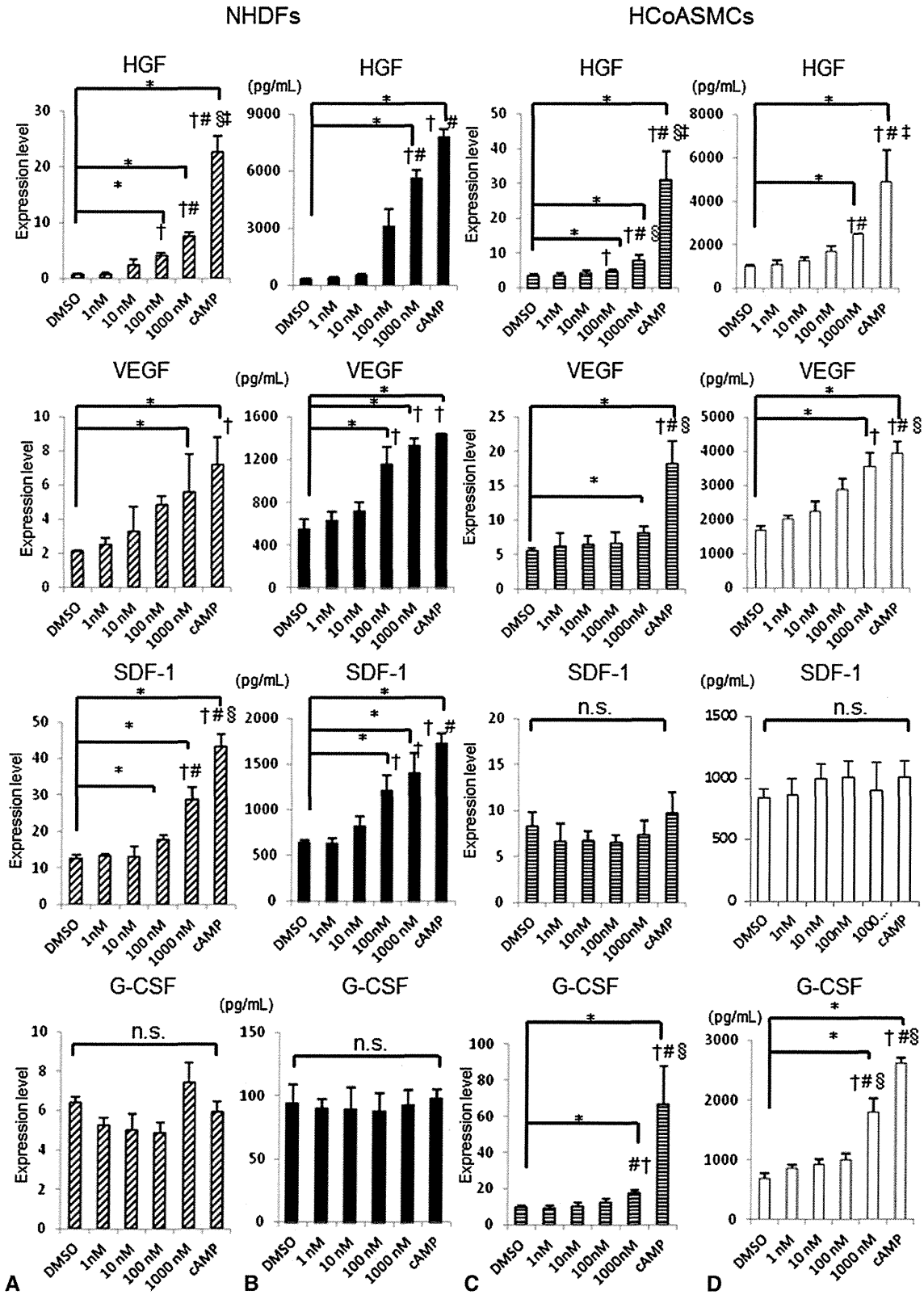

FIGURE 1. Effects of ONO1301 on the production of cardiac protective factors in NHDFs and HCoASMCs were assessed in vitro. ONO1301 treatment significantly upregulates expressions of HGF, VEGF, and SDF-1 in NHDFs, assessed by real-time PCR (A). HGF, VEGF, and SDF-1, but not G-CSF, are significantly secreted into the culture supernatant of NHDF after ONO1301 addition, measured by ELISA (B). ONO1301 addition significantly upregulates expressions of HGF, VEGF, and G-CSF, but not SDF-1, in HCoASMCs, assessed by real-time PCR and ELISA (C and D). *$P < .05$ versus control (DMSO);

the δ-sarcoglycan-deficient DCM hamsters. ONO1301-atelocollagen sheet implantation significantly upregulated expression of HGF, VEGF, increased vasculature, attenuated fibrosis, and upregulated α-sarcoglycan in the myocardium and, consequently, preserved cardiac performance and prolonged survival in this hamster DCM model.

Rationale, Feasibility, and Safety of an Atelocollagen Sheet–Based Therapy for IDCM

This study identified cell-dependent and dose-dependent effects of ONO1301 on the release of cardioprotective factors. The cells that were activated by ONO1301 in vitro included skin fibroblasts and CoASMCs. In addition, IPR, which is the sole receptor of ONO1301, was expressed in CoASMCs and endothelial cells, but not in cardiomyocytes or cardiac fibroblasts. These findings suggest that the target cells of ONO1301 may be the vascular SMCs and endothelial cells in the cardiac tissue. Local delivery of ONO1301 into the heart, directly targeting cardiac SMCs and endothelial cells, would thereby theoretically be useful in maximizing the therapeutic effects of ONO1301. In fact, it was shown that the ONO1301-immersed atelocollagen sheet implantation therapy induced marked heart-dominant elevation of the ONO1301 level in association with significantly positive functional effects, indicating rationale and feasibility of this treatment in the IDCM heart. In addition, both the ONO1301 and the atelocollagen sheet only groups did not produce procedure-related mortality despite the deteriorated cardiac function, suggesting the safety of this treatment for IDCM heart.

There are other possible clinically relevant methods for ONO1301 delivery to treat the DCM heart, such as injection of intramyocardial microbeads, systemic intravenous/subcutaneous injection, or oral intake. However, these methods are theoretically limited by possible local damage and/or poor efficiency in the drug delivery to the cardiac tissue[9] compared with the atelocollagen sheet–based drug delivery system as in this study. Intramyocardial injection of microbeads may also prove to be more efficacious, but further studies will be required to establish the optimal delivery methods of ONO1301 into the heart in preclinical and subsequent clinical studies.

Therapeutic Effects and Underlying Mechanisms of ONO1301 Sheet Therapy

Therapeutic efficiency of this treatment on this δ-sarcoglycan-deficient hamster IDCM model was assured in this study by comparing with the 2 control groups, in which the sham operation or placement of atelocollagen sheet only was performed. Global systolic cardiac function, assessed by echocardiography, was significantly preserved in the ONO1301-treated hamsters compared with the other groups, and most important, the life expectancy of the J2N-k hamsters was prolonged by this treatment. These important positive findings would be explained by multiple fundamental effects of this treatment, including increased myocardial blood flow, reduction of myocardial fibrosis, and reorganization of cytoskeletal proteins.

It has been reported that ONO1301 acts as an inducer of multiple cardioprotective factors in ischemic cardiac diseases.[5] Effects of ONO1301 on the IDCM heart, however, are poorly understood. Although the clinical manifestations of end-stage IDCM are similar to those of end-stage ischemic cardiomyopathy, typical IDCM is characterized by a decreased vascular network, increased fibrous components, and decreased expression of cytoskeletal proteins in a global and homogeneous manner.[10,11] This study also identified multiple endogenous factors upregulated by the ONO1301-atelocollagen sheet, such as HGF, a unique growth factor with antifibrosis and angiogenesis effects,[8,12] or VEGF, an important mediator of angiogenesis.[4] In addition, SDF-1 or G-CSF by the ONO1301 treatment in this study may have contributed to therapeutic stem cell homing and activation.[13,14] Further studies will be required to determine whether these agents induce regenerative responses.

The potential effects of these endogenous factors were well correlated with the pathologic changes in this study, such as increased vasculature, attenuated fibrosis, or upregulated α-sarcoglycan. Of them, increased blood flow may be one of the major mechanisms responsible for the positive therapeutic effects of the ONO1301 in this study. It has been shown that prostacyclin and prostacyclin-inducing HGF/VEGF bring a multiplier effect of vasodilation and new vessel formation responsible to regional ischemic insult.[15,16] In addition, genetic deletion of IPR had an important role on progression of cardiovascular disease.[15]

It is also interesting that cytoskeletal proteins were remodeled by the ONO1301 treatment in this study. Immunohistolabeling in this study demonstrated the transient reexpression of α-sarcoglycan and α-dystroglycan in the O group. It was speculated that α-sarcoglycan can be recycled from the plasma membrane differently from other sarcoglycans,[17] and inhibition of Smad3 associated with transforming growth factor β signal pathway suppressed by prostacyclin or HGF, brings to α-sarcoglycan gene expression.[18]

†$P < .05$ versus ONO1301 (1 nmol/L); #$P < .05$ versus ONO1301 (10 nmol/L); §$P < .05$ versus ONO1301 (100 nmol/L); ‡$P < .05$ versus ONO1301 (1000 nmol/L). *NHDF*, Normal human dermal fibroblast; *HCoASMC*, human coronary artery smooth muscle cell; *HGF*, hepatic growth factor; *VEGF*, vascular endothelial growth factor; *SDF-1*, stromal cell–derived factor-1; *PCR*, polymerase chain reaction; *G-CSF*, granulocyte colony stimulating factor; *ELISA*, enzyme-linked immunosorbent assay; *DMSO*, dimethyl sulphoxide; *cAMP*, cyclic aminophosphatase; *n.s.*, not significant.

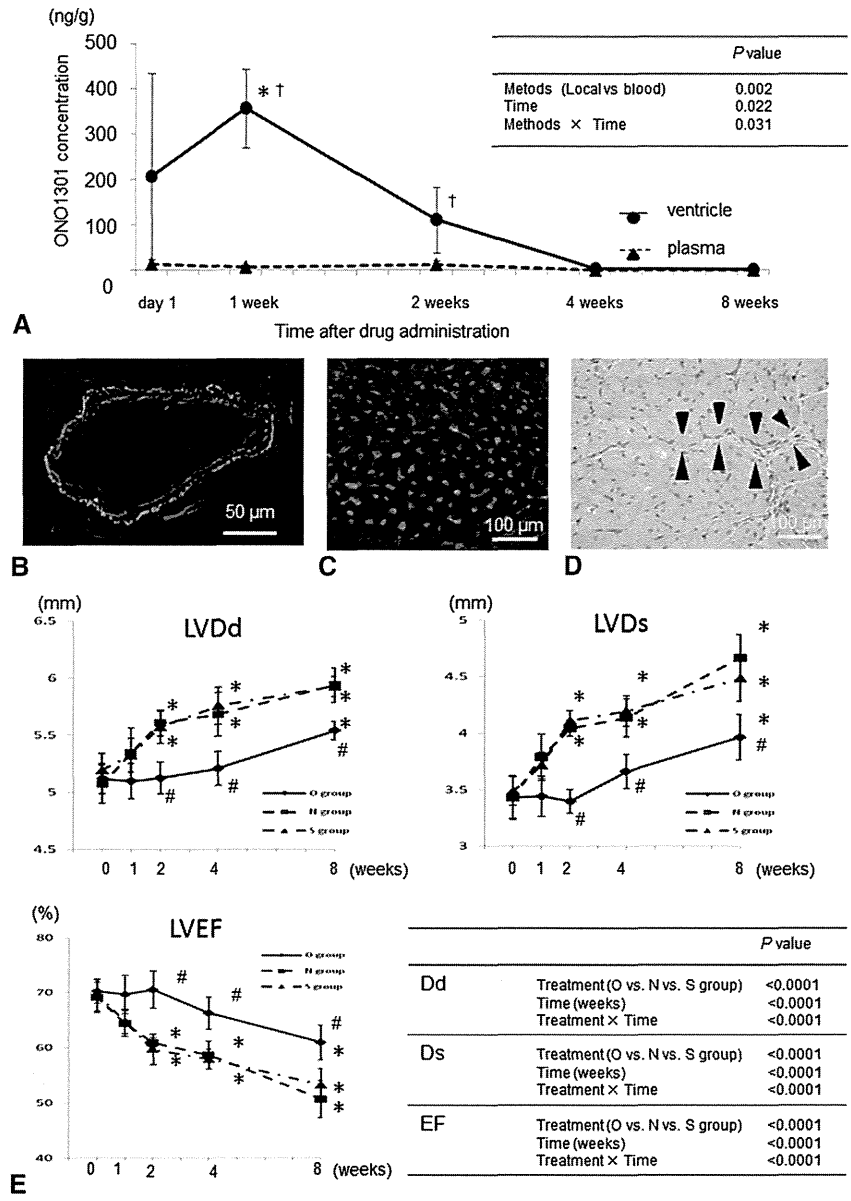

FIGURE 2. Levels of ONO1301 in cardiac tissue and plasma were serially quantified after implantation of ONO1301-eluted atelocollagen sheet for the DCM heart (A). ONO1301 is detected in both samples for 2 weeks after treatment, while the level of ONO1301 in the ventricle is significantly and markedly higher than in the plasma at weeks 1 and 2 after the treatment. *$P < .05$ versus 8 weeks; †$P < .05$ versus plasma concentration Immunofluorescence staining for IPR and alpha-actin in the DCM heart shows that IPR is positive in the vascular smooth muscle cells and the endotherial cells (B and C). *Green*, Filamentous-actin; *red*, IPR; *blue*, nuclei. 3,3′-diaminobenzidine staining, which produces a *brown color*, shows that IPR is expressed in the microvasculature, but not in cardiac fibroblasts and cardiomyocytes (*arrowhead*, cardiac fibroblast) (D). Changes in LVDd/Ds, and LVEF after treatment were serially measured by transthoracic echocardiography (E). These 4 parameters of the LV are preserved until 4 weeks after ONO1301 treatment compared with the other groups. However, ONO1301 treatment does not arrest the progression in dilatation of the dimensions and deterioration of the EF in the subsequent 4 weeks. #$P < .05$ versus N and S group; *$P < .05$ versus 0 weeks. *DCM*, Dilated cardiomyopathy; *LV*, left ventricular (ventricle); *Dd/Ds*, diastolic/systolic dimensions; *EF*, ejection fraction; *IPR*, prostacyclin receptor.

Moreover, regarding the transient reexpression of α-dystroglycan, Kondoh and associates[9] suggested that the reconstruction of α-dystroglycan may occur because the sarcoglycan might mask the matrix metalloproteinase cleavage site on dystroglycan and/or matrix metalloproteinase activity might be inhibited by HGF. In addition, β-sarcoglycan was rarely expressed after the ONO1301 treatment in our study. Kawada and colleagues[19] reported that both β- and δ-sarcoglycan were completely missing, but α- and γ-sarcoglycan were weakly expressed in the J2N-k hamster, and transfer of the δ-sarcoglycan gene could express not only δ- but the other 3 sarcoglycans. These findings might suggest the limitation of this drug therapy for reorganization of cytoskeletal proteins, but Hack and coworkers[20] reported that the

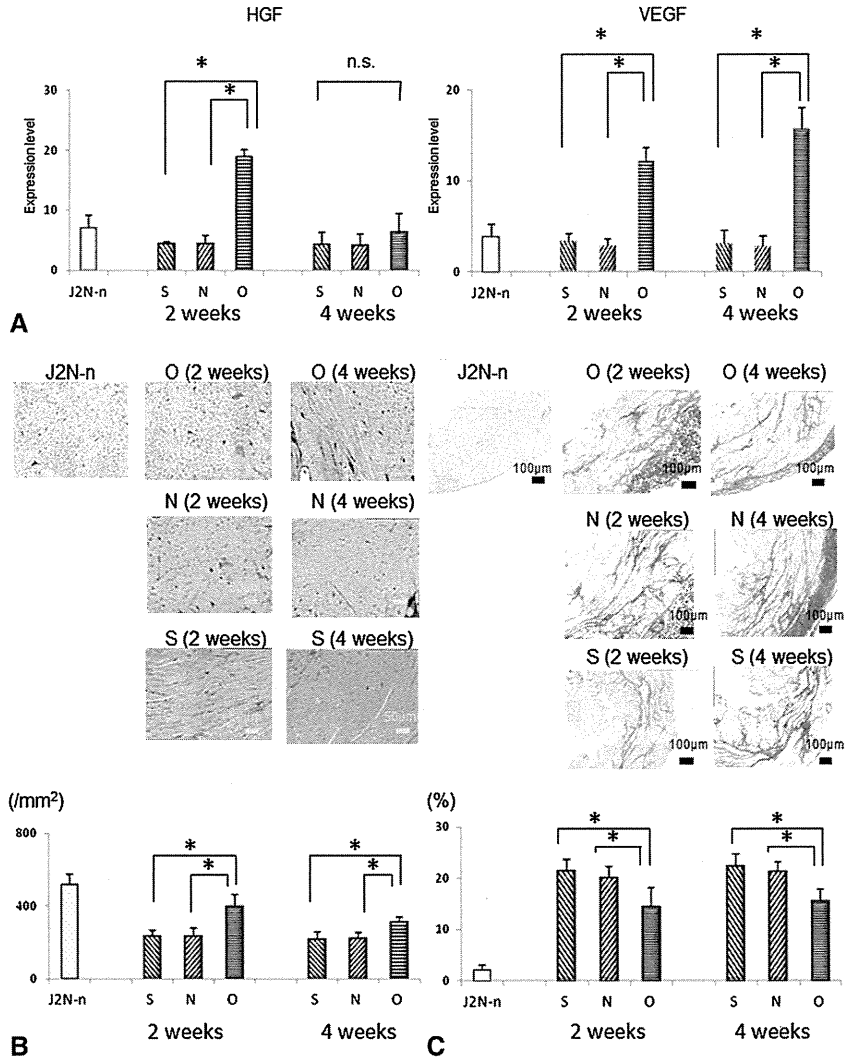

FIGURE 3. Expressions of HGF and VEGF in the cardiac tissue were assessed by real-time PCR, which shows greater expression of the 2 factors in the O group at 2 and 4 weeks compared with the other groups (n = 5 for each group) (A). Capillary density in the hearts was assessed by immunohistolabeling for vWF, which shows a greater number of capillaries in the ONO1301-treated hearts than in the other groups at 2 and 4 weeks (n = 5 for each group) (B). Interstitial fibrosis in the heart was assessed by picrosirius red staining, which shows less accumulation of fibrosis in the ONO1301-treated hearts than in the other groups at 2 and 4 weeks (n = 5 for each group) (C). *$P < .05$ versus O group. *HGF*, Hepatic growth factor; *VEGF*, vascular endothelial growth factor; *PCR*, polymerase chain reaction. *vWF*, von Willebrand factor.

expression of sarcoglycans, even in small amounts, prevented the damage of cardiomyocyte. Reorganization of α-sarcoglycan by the ONO1301 therapy might thus contribute to preserve cardiac function.

Although the level of prostacyclin in the heart in response to the ONO1301 treatment was not investigated in this study, it may be paradoxically elevated by the thromboxane synthase inhibitory activity of the ONO1301 on the heart,[21] possibly producing synergetic positive effects on the IDCM heart. In addition, it is interesting to research the involvement of the neurohormonal activations in the heart, such as adrenergic system, plasma renin activity, or endothelin, by the ONO1301 treatment.[22]

Clinical Perspectives

The atelocollagen sheet–based local ONO1301 delivery therapy globally reversed reduced vascular density, increased fibrosis, and reduced cytoskeletal proteins in the myocardium, all of which were the typical pathologic features in the human IDCM heart,[10,11] suggesting potential therapeutic benefits of this treatment for IDCM in the clinical scenario. In addition, safety of this treatment shown in this study warrants further preclinical study, including dose-response relation to explore minimum and maximal effective dose of the ONO1301 in the "GLP" standard. A very narrow dose necessary to achieve a positive response may prohibit this agent from clinical trials.

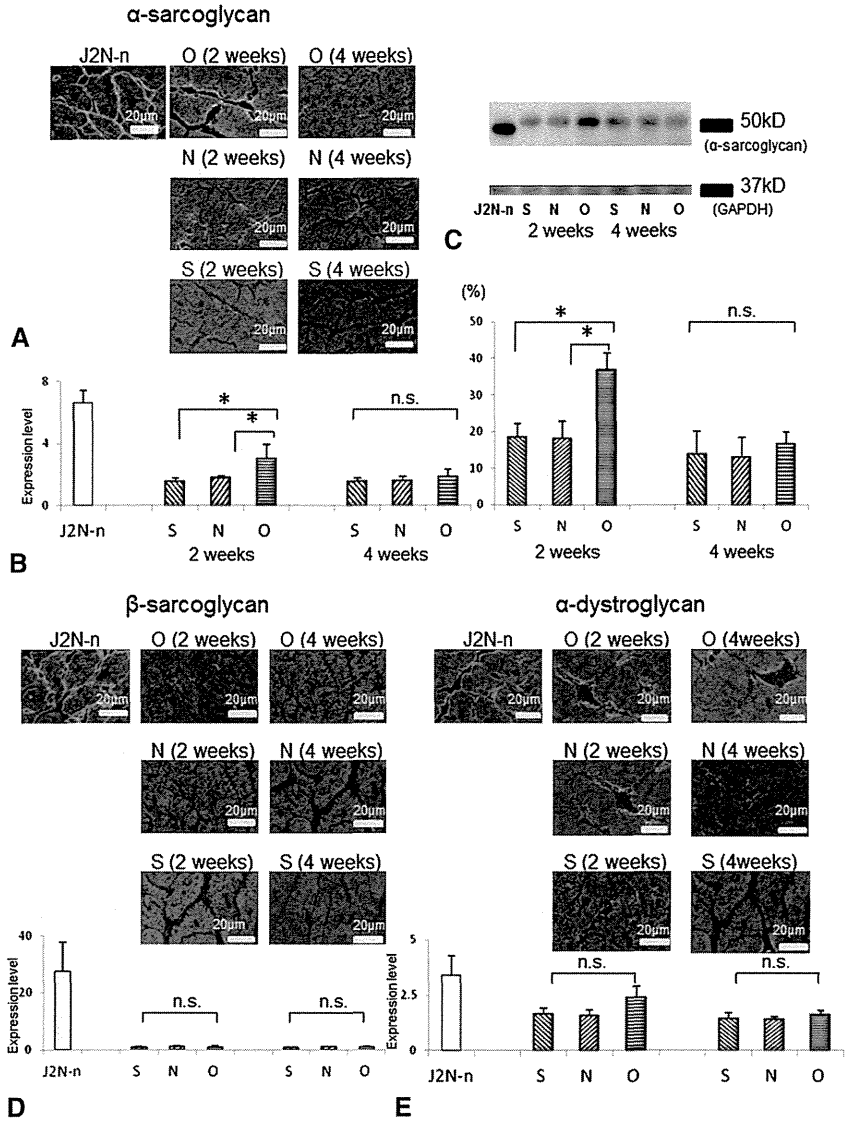

FIGURE 4. Expression of α-sarcoglycan, β-sarcoglycan, and α-dystoglycan in the heart after ONO1301 treatment was assessed by immunohistolabeling, real-time PCR, and Western blot analysis. Immunohistolabeling shows that α-sarcoglycan is clearly expressed around the cardiomyocytes in the normal hamsters, but not in the N or S group (A). Of note, α-sarcoglycan is expressed in the O group at 2 weeks but not at 4 weeks. *Green*, α-Sarcoglycan; *red*, filamentous-actin; *blue*, nuclei. Quantitative real-time PCR shows a significantly greater expression of α-sarcoglycan in the O group than in the N or S group at 2 weeks, but not at 4 weeks (n = 5 for each group at each time point, $*P < .05$ vs O group) (B). Consistently, Western blot analysis and the quantitative results of band intensities, which are expressed as a percentage of the value of the J2N-n hamsters, show significantly greater expression of α-sarcoglycan in the O group than in the N or S group at 2 weeks, but not at 4 weeks (n = 5 for each group at each time point, $*P < .05$ vs O group) (C). Expression of β-sarcoglycan in the DCM hamsters is not detected even after ONO1301 treatment (D). *Green*, β-sarcoglycan; *red*, filamentous-actin; *blue*, nuclei. α-Dystroglycan is rarely expressed in the N or S group, although its expression is upregulated in the O group (E). There are no significant differences between the O group and the other groups at 2 weeks. *Green*, α-Dystroglycan; *red*, filamentous-actin; *blue*, nuclei. *PCR*, Polymerase chain reaction; *n.s.*, not significant.

Re-treatment of epicardial implantation of the sheet containing ONO1301 might be technically challenging; however, technical modulation of microsphere generation, such as gelatin hydrogel, might induce further developments to generate a longer-release drug-delivery system than the method used in the present study.[23]

Study Limitations

This study was limited by use of a transgenic rodent model. The δ-sarcoglycan-deficient IDCM model used in this study is not completely relevant to human IDCM that shows a number of etiologic and pathologic variations. However, positive functional and pathologic effects

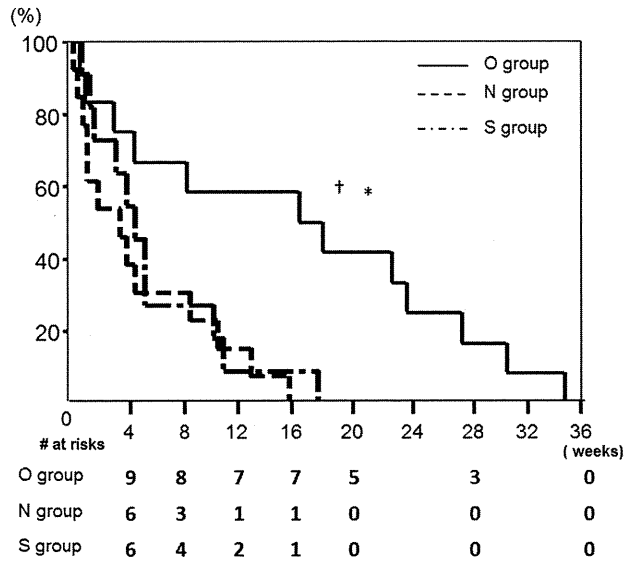

FIGURE 5. Survival after treatment was assessed by the Kaplan-Meier method. There is no significant difference between the N (n = 11) and S groups (n = 13), whereas the O group (n = 12) shows a significantly greater survival than the other groups (*$P < .05$ vs S group; †$P < .05$ vs N group).

associated with upregulated protective factors would be sufficient to prove the principal concept of this treatment. Agents that are beneficial in these mutant hamsters may not be beneficial in humans because the mechanisms responsible for the beneficial effects may be different in humans. However, further pathologic and functional studies for human DCM heart samples, in comparison with the deficient hamster, may be useful to strengthen the findings of this study.

Poor availability of the antibodies and genome sequences in the hamster limited in-depth evaluation of the mechanisms responsible for this treatment, which is warranted to be supplemented by murine IDCM model.[24]

CONCLUSIONS

ONO1301 reorganized cytoskeletal proteins, especially α-sarcoglycan, increased capillaries, and reduced fibrosis through the upregulation of cardiac protective factors, leading to functional recovery and prolonged survival in the δ-sarcoglycan-deficient IDCM hamster. A preclinical study to explore the optimal, clinically relevant protocol is warranted.

We thank Masako Yokoyama, Akima Harada, and Motoko Shiozaki for their excellent technical assistance.

References

1. Rajnoch C, Chachques JC, Berrebi A, Bruneval P, Benoit MO, Carpentier A. Cellular therapy reverses myocardial dysfunction. *J Thorac Cardiovasc Surg.* 2001; 121:871-8.
2. Nakamura T, Matsumoto K, Mizuno S, Sawa Y, Matsuda H, Nakamura T. Hepatocyte growth factor prevents tissue fibrosis, remodeling, and dysfunction in cardiomyopathic hamster hearts. *Am J Physiol Heart Circ Physiol.* 2005;288:H2131-9.
3. Juan CC. Cellular cardiac regenerative therapy in which patients? *Expert Rev Cardiovasc Ther.* 2009;7:911-9.
4. Matsumoto K, Okazaki H, Nakamura T. Novel function of prostaglandins as inducers of gene expression of HGF and putative mediator of tissue regeneration. *J Biochem.* 1995;117:458-64.
5. Iwata H, Nakamura K, Sumi M, Ninomiya M, Sakai Y, Sata M, et al. Local delivery of synthetic prostacycline agonist augments collateral growth and improves cardiac function in a swine chronic cardiac ischemia model. *Life Sci.* 2009;85:255-61.
6. Mitsuhashi S, Saito N, Watano K, Igarashi K, Tagami S, Kikuchi K, et al. Defect of Delta-sarcoglycan gene is responsible for development of dilated cardiomyopathy of a novel hamster strain, J2N-k: calcineurin/PP2B activity in the heart of J2N-k hamster. *J Biochem.* 2003;134:269-76.
7. Saini SG, Wani AT, Vashney B, Ahmed T, Rajan SK, Paliwal LJ. Validation of the LC-MS/MS method for the quantification of mevalonic acid in human plasma and determination of the matrix effect. *J Lipid Res.* 2006;47:2340-5.
8. Miyagawa S, Sawa Y, Taketani S, Kawaguchi N, Nakamura T, Matsuda H, et al. Myocardial regeneration therapy for heart failure: hepatocyte growth factor enhances the effect of cellular cardiomyoplasty. *Circulation.* 2002; 105:2556-61.
9. Kondoh H, Sawa Y, Miyagawa S, Matsumiya S, Sakakida-Kitagawa S, Matsuda H, et al. Longer preservation of cardiac performance by sheet-shaped myoblast implantation in dilated cardiomyopathic hamsters. *Cardiovasc Res.* 2006;69:466-75.
10. Neglia D, Michelassi C, Trivieri MG, Sambuceti G, Giorgetti A, Parodi O, et al. Prognostic role of myocardial blood flow impairment in idiopathic left ventricular dysfunction. *Circulation.* 2002;105:186-93.
11. Towbin JA. The role of cytoskeletal proteins in cardiomyopathies. *Curr Opin Cell Biol.* 1998;10:131-9.
12. Taniyama Y, Morishita R, Aoki M, Hirooka K, Yamasaki K, Ogihara T, et al. Angiogenesis and antifibrotic action by hepatocyte growth factor in cardiomyopathy. *Hypertension.* 2002;40:47-53.
13. Saxena A, Fish JE, White MD, Yu S, Smyth JW, Srivastava D, et al. Stromal cell–derived factor-1α is cardioprotective after myocardial infarction. *Circulation.* 2008;117:2224-31.
14. Stanford SJ, Pepper JR, Mitchell JA. Release of GM-CSF and G-CSF by human arterial and venous smooth muscle cell: differential regulation by COX-2. *Br J Pharmacol.* 2000;129:835-8.
15. Fetalvero KM, Martin KA, Hwa J. Cardioprotective prostacyclin signaling in vascular smooth muscle cell. *Prostaglandins Other Lipid Mediat.* 2007;82: 109-18.
16. Hiraoka K, Koike H, Yamamoto S, Tomita N, Yokoyama C, Morishita R, et al. Enhanced therapeutic angiogenesis by cotransfection of prostacyclin synthase gene or optimization of intramuscular injection of naked plasmid DNA. *Circulation.* 2003;108:2689-96.
17. Draviam RA, Wang B, Shand SH, Xiao X, Watkins SC. Alpha-sarcoglycan is recycled from the plasma membrane in the absence of sarcoglycan complex assembly. *Traffic.* 2006;7:793-810.
18. Hernández-Hernández JM, Delgado-Olguín P, Aguillón-Huerta V, Furlan-Magaril M, Recillas-Targa F, Coral-Vázquez RM. Sox9 represses alpha-sarcoglycan gene expression in early myogenic differentiation. *J Mol Biol.* 2009;394:1-14.
19. Kawada T, Nakaturu Y, Sakamoto A, Koizumi T, Shin WS, Toyooka T, et al. Strain- and age-dependent loss of sarcoglycan complex in cardiomyopathic hamster hearts and its re-expression by delta-sarcoglycan gene transfer in vivo. *FEBS Lett.* 1999;458:405-8.
20. Hack AA, Lam MY, Cordier L, Shoturma DI, Ly CT, Hadhazy MA. Differential requirement for individual sarcoglycans and dystrophin in the assembly and function of the dystrophin-glycoplotein complex. *J Cell Sci.* 2000; 113:2535-44.
21. Yamanaka S, Miura K, Yukimura T, Okumura M, Yamamoto K. Putative mechanism of hypotensive action of platelet-activating factor in dogs. *Circ Res.* 1992; 70:893-901.
22. Somova LI, Mufunda JJ. Renin-angiotensin-aldosterone system and thromboxane A2/prostacyclin in normotensive and thromboxane A2/prostacyclin in normotensive and hypertensive black Zimbabweans. *Ethn Dis.* 1992;2:27-34.
23. Takaoka R, Hikasa Y, Hayashi K, Tabata Y. Bone regeneration by lactoferrin released from a gelation hydrogel. *J Biomater Sci Polym Ed.* 2010;22:1581-9.
24. Lu D, Ma Y, Zhang W, Bao D, Dong W, Zhang L, et al. Knockdown of cytochrome P450 2E1 inhibits oxidative stress and apoptosis in the cTnT (R141W) dilated cardiomyopathy transgenic mice. *Hypertension.* 2012;60:81-9.

PLOS ONE

Sustained-Release Delivery of Prostacyclin Analogue Enhances Bone Marrow-Cell Recruitment and Yields Functional Benefits for Acute Myocardial Infarction in Mice

Yukiko Imanishi[1], Shigeru Miyagawa[1], Satsuki Fukushima[1], Kazuhiko Ishimaru[1], Nagako Sougawa[1], Atsuhiro Saito[2], Yoshiki Sakai[3], Yoshiki Sawa[1]*

1 Department of Cardiovascular Surgery, Graduate School of Medicine, Osaka University, Osaka, Japan, **2** Medical Center for Translational Research, Osaka University Hospital, Osaka, Japan, **3** Research Headquarters, ONO Pharmaceutical CO., LTD., Osaka, Japan

Abstract

Background: A prostacyclin analogue, ONO-1301, is reported to upregulate beneficial proteins, including stromal cell derived factor-1 (SDF-1). We hypothesized that the sustained-release delivery of ONO-1301 would enhance SDF-1 expression in the acute myocardial infarction (MI) heart and induce bone marrow cells (BMCs) to home to the myocardium, leading to improved cardiac function in mice.

Methods and Results: ONO-1301 significantly upregulated SDF-1 secretion by fibroblasts. BMC migration was greater to ONO-1301-stimulated than unstimulated conditioned medium. This increase was diminished by treating the BMCs with a CXCR4-neutralizing antibody or CXCR4 antagonist (AMD3100). Atelocollagen sheets containing a sustained-release form of ONO-1301 (n = 33) or ONO-1301-free vehicle (n = 48) were implanted on the left ventricular (LV) anterior wall immediately after permanent left-anterior descending artery occlusion in C57BL6/N mice (male, 8-weeks-old). The SDF-1 expression in the infarct border zone was significantly elevated for 1 month in the ONO-1301-treated group. BMC accumulation in the infarcted hearts, detected by in vivo imaging after intravenous injection of labeled BMCs, was enhanced in the ONO-1301-treated hearts. This increase was inhibited by AMD3100. The accumulated BMCs differentiated into capillary structures. The survival rates and cardiac function were significantly improved in the ONO-1301-treated group (fractional area change 23±1%; n = 22) compared to the vehicle group (19±1%; n = 20; P = 0.004). LV anterior wall thinning, expansion of infarction, and fibrosis were lower in the ONO-1301-treated group.

Conclusions: Sustained-release delivery of ONO-1301 promoted BMC recruitment to the acute MI heart via SDF-1/CXCR4 signaling and restored cardiac performance, suggesting a novel mechanism for ONO-1301-mediated acute-MI heart repair.

Citation: Imanishi Y, Miyagawa S, Fukushima S, Ishimaru K, Sougawa N, et al. (2013) Sustained-Release Delivery of Prostacyclin Analogue Enhances Bone Marrow-Cell Recruitment and Yields Functional Benefits for Acute Myocardial Infarction in Mice. PLoS ONE 8(7): e69302. doi:10.1371/journal.pone.0069302

Editor: Toru Hosoda, Tokai University, Japan

Received February 8, 2013; **Accepted** June 6, 2013; **Published** July 19, 2013

Funding: This study was funded by grant-in-aid for Core-to-Core Program (21003) from the Japan Society for the Promotion of Science (http://jsps-osaka-u.jpn.org/en/index.html), early-stage and exploratory clinical trial centers project from the Ministry of Health (http://jsps-osaka-u.jpn.org/en/index.html), Labour and Welfare, Health and Labour Sciences Research Grant (H23-002, http://jsps-osaka-u.jpn.org/en/index.html), and from New Energy and Industrial Technology Development Organization (P10004, http://www.nedo.go.jp/english/index.html). The funders had no role in study design, data collection and analysis, decision to publish, or preparation of the manuscript.

Competing Interests: The authors have read the journal's policy and have the following conflicts: Y. Sakai was an employee of Ono Pharmaceutical Co. Ltd., and a holder of the patent for ONO-1301 encapsulated in PLGA microspheres (patent numbers WO 2004/032965 and WO 2008/047863). There are no other patents, products in development, or modified products to declare. The other authors have declared that no competing interests exist. This does not alter the authors' adherence to all PLOS ONE policies on sharing data and materials.

* E-mail: sawa@surg1.med.osaka-u.ac.jp

Introduction

Despite a number of medical and interventional treatments have been developed to treat acute myocardial infarction (AMI), the treatment for massive AMI has not been fully established. Myocardial infarction (MI) is a progressive disease, characterized by massive ischemic necrosis of the myocardial tissue and subsequent inflammation. This leads to cardiac remodeling that exacerbates the oxygen shortage in the surviving cardiac tissue. These pathological and functional deteriorations eventually cause end-stage heart failure. To delay the progression of heart failure, it is essential to suppress inflammation and fibrosis and to improve bloodflow supply in the injured myocardium consecutively. Recently, stromal cell-derived factor (SDF)-1 and its corresponding receptor CXCR4 have been shown to play prominent roles in homing of bone marrow cells (BMC) which promotes neovascularization and prevention of apoptosis via paracrine mechanism [1,2,3,4].

ONO-1301 (({5-[2-({[(1E)-phenyl(pyridin-3-yl)methylene]amino}oxy)ethyl]-7,8-dihydronaphthalen-1-yl}oxy)acetic acid) is a synthetic prostacyclin agonist. As it lacks the typical prostanoid

structure of a five-membered ring and an allylic alchol, ONO-1301 is chemically and biologically stable *in vivo*. In addition, thromboxane A2 synthethase is inhibited by ONO-1301, resulting in the promotion of endogenous prostacyclin synthesis. ONO-1301 has been reported to induce the production of endogenous hepatocyte growth factor (HGF) and vascular-endothelial growth factor (VEGF) in fibroblasts by stimulating cAMP production [5,6,7,8]. The administration of a slow-release form of ONO-1301 shows therapeutic potential, mainly due to the restoration of bloodflow in MI models of rat and swine and in a cardiomyopathic hamster [6,7,8]. The potential mechanism of the functional benefits of ONO-1301 mainly result from the enhanced secretion of growth factors, such as HGF and VEGF, which induce angiogenesis, restore bloodflow, and attenuate the progression of fibrosis. Recently we identified that ONO-1301 also upregulates SDF-1 secretion in the fibroblasts. Enhanced BMC homing in the MI heart by ONO-1301 therapy is attractive therapeutic modality. We thus hypothesized that ONO-1301 can induce BMC accumulation mediated by the upregulation of SDF-1 to elicit functional improvement in a mouse model of MI.

Methods

This study was carried out in strict accordance with the recommendations in the Guide for the Care and Use of Laboratory Animals of the National Institutes of Health. The protocol was approved by the Committee on the Ethics of Animal Experiments of the Osaka University (H23–123). All surgery was performed under sodium pentobarbital or isoflurane anesthesia, and all efforts were made to minimize suffering.

ONO-1301 and a slow-release form of ONO-1301 were purchased from ONO Pharmaceutical Co. Ltd. (Osaka, Japan) [7,8,9].

Migration Assay

Normal human dermal fibroblasts (NHDFs; Takara bio, Shiga, Japan) were cultured with or without ONO-1301 for 72 hours. The SDF-1 concentration in the culture supernatants was measured by ELISA (R&D systems, MN). BMCs were obtained from a green fluorescent protein (GFP)-transgenic mouse [C57BL/6-Tg(CAG-EGFP); Japan SLC, Inc., Shizuoka, Japan], and their migration toward the supernatants was assessed using a culture insert system (BD Falcon). The number of migrated BMCs was determined using fluorescence microscopy (Carl Zeiss, Göttingen, Germany).

Mouse AMI Model and Sheet Transplantation

An AMI model was generated by permanent ligation of the left anterior descending artery (LAD) in 10-15-week-old male C57BL/6N, BALB/cA, or BM-GFP chimera mice [10]. ONO-1301 microspheres and control microspheres were resuspended in saline at 10 mg/ml and added to atelocollagen sheets just before transplantation. Five minutes after the LAD ligation, atelocollagen sheets that included ONO-1301-containing microspheres (ONO-1301-treated group, n = 40) or empty microspheres (vehicle group, n = 40) were fixed onto the surface of the anterior left ventricular (LV) wall. The mice were euthanized 7, 21, and 28 days after the LAD ligation and ONO-1301 administration.

Assessment of BMC Homing

BMCs harvested from BALB/cA mice were labeled by Xenolight DiR (Caliper Life Sciences, MA) following the manufacturer's instructions and injected into the tail vein of BALB/cA mice after the MI and ONO-1301 treatment. On days 1 and 3, the whole-body imaging of the mice was measured by an *in vivo* imaging system (IVIS, Caliper Life Sciences).

Assessment of Cardiac Function and Survival

Cardiac function was assessed using an echocardiography system equipped with a 12-MHz transducer (GE Healthcare, WI) 4 weeks after MI and ONO-1301 treatment. The LV areas were measured, and LV fractional area change (FAC) was calculated as (LVEDA-LVESA)/LVEDA×100, where LVEDA and LVESA are the LV end-diastolic and end-systolic area, respectively.[10] The mice were housed in a temperature-controlled incubator for 28 days post-treatment to determine their survival.

Histological Analysis

Frozen sections (8 μm) of hearts were stained with antibodies against von Willebrand factor (vWF; Dako, Glostrup, Denmark) and CD31 (Abcam, UK). The secondary antibody was Alexa 546 goat anti-rabbit (Life Technologies, CA). Counterstaining was performed with 6-diamidino-2-phenylindole (DAPI; Life Technologies). The sections were also stained with isolectin (Life Technologies) following the manufacturer's instructions. To count GFP-positive cells, isolectin-positive cells, and CD31-positive capillary densities, 10 images were captured for each specimen. Capture and analysis were performed using Biorevo (Keyence, Japan). To analyze the myocardial collagen accumulation, heart sections were stained with Masson's trichrome. The collagen volume fraction in the peri-infarct area was calculated.

Quantitative Real-time PCR

The total RNA was isolated from the peri-infarct area using the RNeasy Mini Kit and reverse transcribed using Omniscript Reverse transcriptase (Qiagen, Hilden, Germany). Quantitative PCR was performed with a PCR System (Life Technologies). The expression of each mRNA was normalized to that of glyceraldehyde-3-phosphate dehydrogenase (GAPDH). The primers and probes are shown in Table S1 in File S1.

Statistical Analysis

Data are expressed as the mean ± SEM. The data distributions were checked for normality. Comparisons between 2 groups were made using the Student's *t*-test. For comparisons among 3 or more groups, one-way analysis of variance (ANOVA) followed by Fisher's protected least significant difference (PLSD) test were used. The survival curves were prepared using the Kaplan-Meier method and compared using the log-rank test. All *P*-values are two-sided, and values of $P<0.05$ were considered to indicate statistical significance. Statistical analyses were performed using the StatView 5.0 Program (Abacus Concepts, Berkeley, CA) and Statcel2 (The Publisher OMS Ltd., Saitama, Japan).

An expanded Methods section can be found in the online-only in File S1.

Results

ONO-1301 Enhanced BMC Migration via SDF-1/CXCR4 Signaling

The effect of ONO-1301 on the SDF-1 secretion by NHDFs was evaluated by ELISA. As shown in Fig. 1A, the SDF-1 concentration in the NHDF culture supernatants increased in an ONO-1301 concentration-dependent manner. The SDF-1 concentration in the culture supernatant of 1000 nM ONO-1301-treated cells was significantly greater than that of cells cultured in

the absence of ONO-1301 (Fig. 1A). To investigate the BMC migration toward ONO-1301-treated NHDF conditioned medium, a migration assay was performed using a modified Boyden chamber with 8-μm pores. The number of migrated BMCs was significantly greater in the conditioned medium of cells treated with 100 and 1000 nM ONO-1301 compared to that of cells treated with 0 and 10 nM ONO-1301. The BMC migration to the 1000 nM ONO-1301 conditioned medium was diminished by treating the BMCs with a CXCR4-neutralizing antibody or CXCR4 antagonist (AMD3100) (Fig. 1B, C).

SDF-1-mediated BMC Accumulation in the ONO-1301-treated Infarcted Hearts

The effect of ONO-1301 on SDF-1 expression in the infarcted hearts was evaluated by quantitative RT-PCR. Twenty-eight days after treatment, the SDF-1 expression in the border area of the ONO-1301-treated heart was significantly greater than that in the vehicle-treated heart (Fig. 2A). The HGF and VEGF expressions were also increased by ONO-1301 treatment (Fig. 2B, C). After LAD occlusion, ONO-1301 treatment, and intravenous injection of labeled BMCs, the BMC accumulation in the infarcted heart was evaluated by an in vivo imaging system. The proportion of BMCs in the heart showed a trend toward upregulation, dependent on the dose of ONO-1301 (Fig. 2D). Hearts treated with 100 mg ONO-1301/kg body weight showed significantly more accumulated BMCs than those treated with 0 or 10 mg ONO-1301. In 100 mg/kg ONO-1301-treated hearts, CXCR4 antagonization significantly decreased the BMC accumulation (Fig. 2D). To identify the recruited BMCs *in vivo*, the acute MI model was prepared using chimera mice by transplanting GFP-expressing bone marrow into irradiated C57BL/6 mice. The BMCs of the C57BL/6 transplant recipients were largely replaced by GFP-expressing BMCs (91.8+/−4.3%, figure S1 in File S1). The single-organ analyses using GFP-BM chimera mouse at day 7 also showed increased BMC accumulation in the ONO-1301-treated myocardium (figure S2 in File S1).

Differentiation of BMCs in the Infarcted Myocardium

Seven days after MI and ONO-1301 administration to BM-GFP chimera mouse, BMCs were dramatically accumulated in both the infarcted area and the atelocollagen sheet (Fig. 3A, B). Some of the BMCs formed tube-like structures and displayed von Willebrand factor expression (Fig. 3C, D). Isolectin staining showed that a greater percentage of isolectin-positive BMCs accumulated in the myocardium in the ONO-1301-treated (O) group than in the vehicle (V) group (Fig. 3E, F). We also evaluated small blood vessels by CD31 immunostaining. The density of small vessels was greater in the O group than in the V group (Fig. 3G). Immunohistochemical analysis of Connexin 43 and smooth muscle actin, cardiac-lineage and cardiac fibroblast markers, respectively, was also conducted at 3 months, but no co-expression

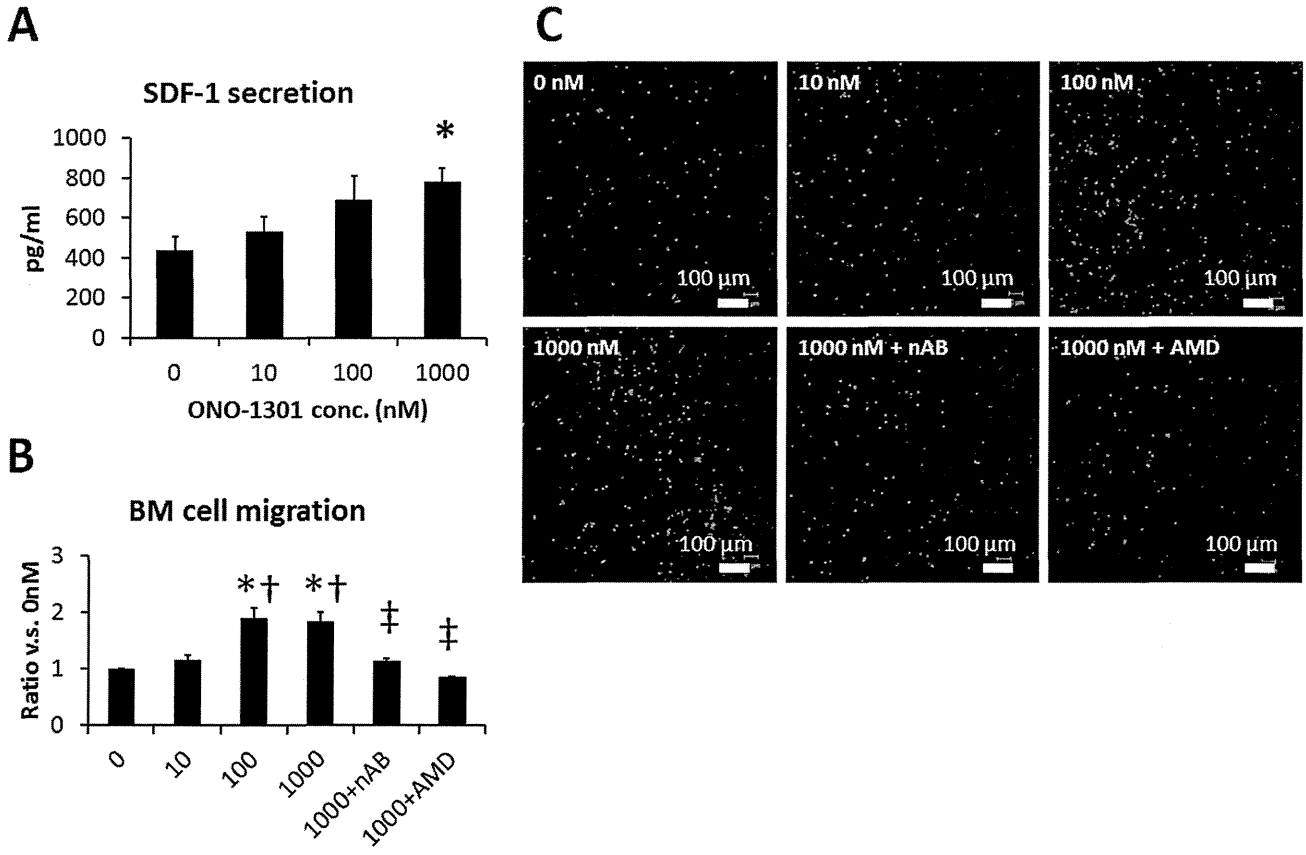

Figure 1. ONO-1301 enhanced SDF-1 secretion and BMC migration via SDF-1/CXCR4 signaling *in vitro*. NHDFs were stimulated with ONO-1301 for 72 hours, then the SDF-1 concentration in the culture medium was determined by ELISA (n = 3 each, *$P<0.05$ vs. 0 nM). A) Number of BMCs that migrated toward the conditioned medium from ONO-1301-stimulated-NHDFs (0, 10, 100, or 1000 nM ONO-1301, n = 6; 1000 nM+nAB or 1000 nM+AMD, n = 3). *$P<0.05$ vs. 0 nM, †$P<0.05$ vs. 10 nM, ‡$P<0.05$ vs. 1000 nM, §$P<0.05$ vs. SDF-1. nAB, CXCR4-neutralizing antibody; AMD, CXCR4 antagonist AMD3100. B) Representative pictures of BMCs that had migrated to the medium from ONO-1301-stimulated BMCs. Green, BMCs.
doi:10.1371/journal.pone.0069302.g001

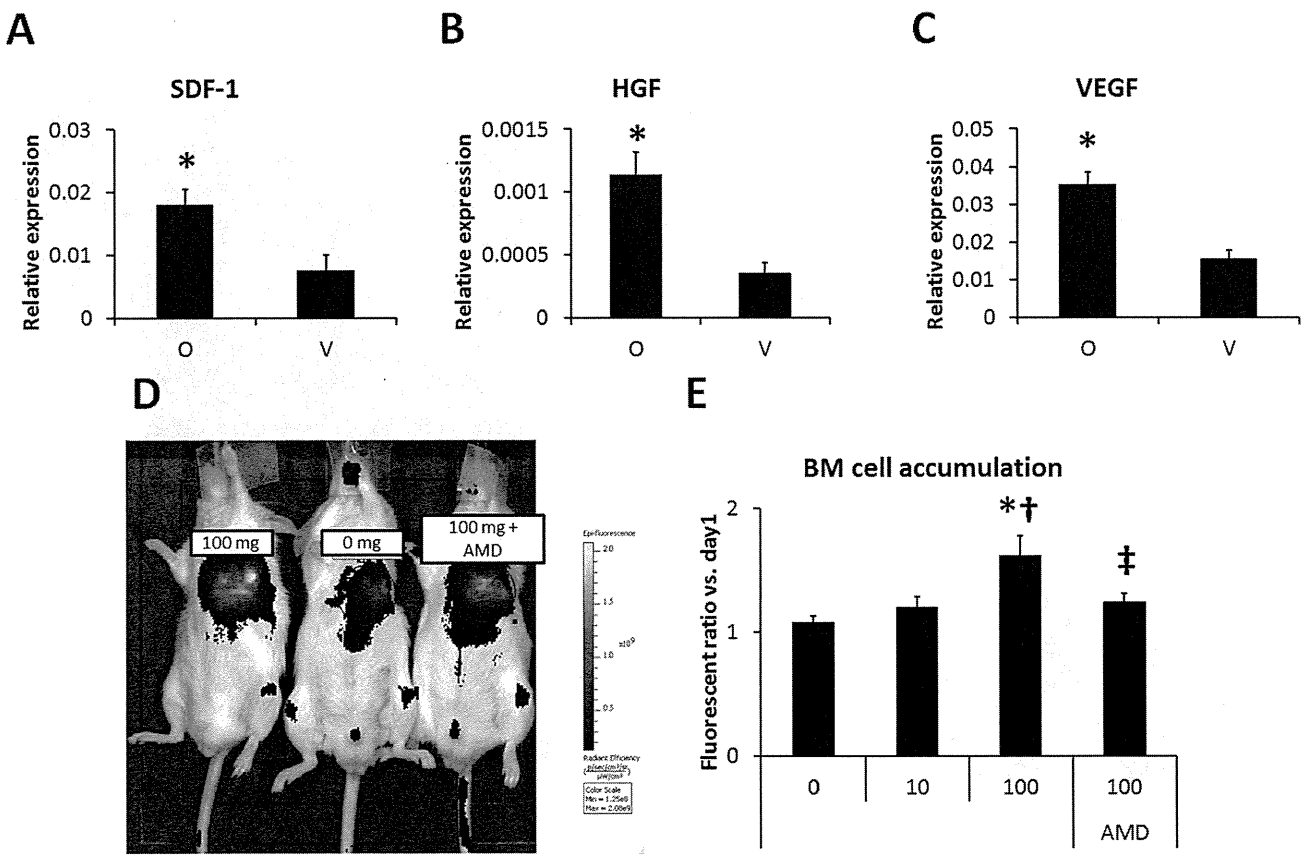

Figure 2. ONO-1301 enhanced SDF-1 secretion and BMC migration via SDF-1/CXCR4 signaling after MI. A–C) The SDF-1, HGF, and VEGF expression at the border zone of the infarcted area was measured by quantitative RT-PCR. The expression levels of these cytokines were higher in the ONO-1301-treated (O) group compared to the vehicle (V) group. (O group, n = 7; V group, n = 7–8; *$P<0.05$ vs. V group). The expression relative to GAPDH is shown. D) BMC migration to ONO-1301-treated infarcted myocardium was evaluated using IVIS. Representative picture of IVIS at day 3. Left: 100 mg/Kg, Center: 0 mg/Kg, Right: 100 mg/Kg+AMD3100 (AMD). E) The number of accumulated BMCs was greater in the 100 mg/kg ONO-1301-treated infarcted heart compared to the 0 and 10 mg/kg ONO-1301-treated infarcted heart. When BMCs treated with AMD were injected, the BMC accumulation decreased in the 100 mg/Kg ONO-1301-treated infarcted heart compared with the untreated-BMC-injected heart (0 mg/Kg, n = 4; 10 mg/Kg, n = 8; 100 mg/Kg, n = 5; 100 mg/Kg+AMD3100, n = 4; *$P<0.05$ vs. 0 mg/Kg, †$P<0.05$ vs. 10 mg/Kg, ‡$P<0.05$ vs. 100 mg/Kg).
doi:10.1371/journal.pone.0069302.g002

of GFP with either of these markers was observed (figure S3 in File S1).

Therapeutic Effects of ONO-1301 Administration on Cardiac Performance, Survival, and LV-remodeling at 4 Weeks Post-MI

ONO-1301 was detected in the plasma of blood samples from the ONO-1301-treated group 3 weeks after treatment (figure S4 in File S1). The cardiac functions in the MI mice with and without following ONO-1301 treatment were evaluated. Mortality was substantial until 14 days post-LAD ligation in the vehicle group, and similar mortality levels were observed with non-treated MI mice [11]. In contrast, in the ONO-1301-treated group, there was little mortality 7 days after MI, and thus a difference in survival (Fig. 4A). Cardiac performance was evaluated by 2D echocardiography 4 weeks after implantation. The LVEDA was smaller in the ONO-1301-treated group than in the vehicle group, but the difference was not significant. In contrast, the LVESA was significantly smaller, and the LVFAC was significantly greater, in the ONO-1301-treated group than in the vehicle group (Fig. 4B). In the histological analysis, the vehicle group showed a typical MI with a large anterior LV scar and dilatation of the LV cavity. By comparison, the LV of the ONO-1301-treated group was less dilated, and the anterior wall was thicker (Fig. 4C, D). The infarcted area and percent fibrosis were significantly smaller in the ONO-1301-treated than in the vehicle-treated group (Fig. 4C, E–G).

Discussion

Here, we showed that ONO-1301 promotes BMC accumulation in the injured myocardium. *In vitro*, ONO-1301 enhanced SDF-1 expression, and BMC migration was greater to conditioned medium obtained from ONO-1301-stimulated cells. The enhanced migration was diminished by blocking SDF-1/CXCR4 signaling. Consistent with the *in vitro* experiments, ONO-1301 enhanced the SDF-1 expression of myocardial tissue. High ONO-1301 accelerated the BMC accumulation after MI in a SDF-1/CXCR4-dependent manner. Some BMCs in the infarcted myocardium differentiated into capillary structures within 7 days. Furthermore, the sustained-release delivery of ONO-1301 in the infarcted myocardium also led to functional improvements following MI. Our data suggest that ONO-1301 is a novel inducer of BMC recruitment, and that ONO-1301 treatment may be a promising therapeutic strategy for the clinical treatment of MI.

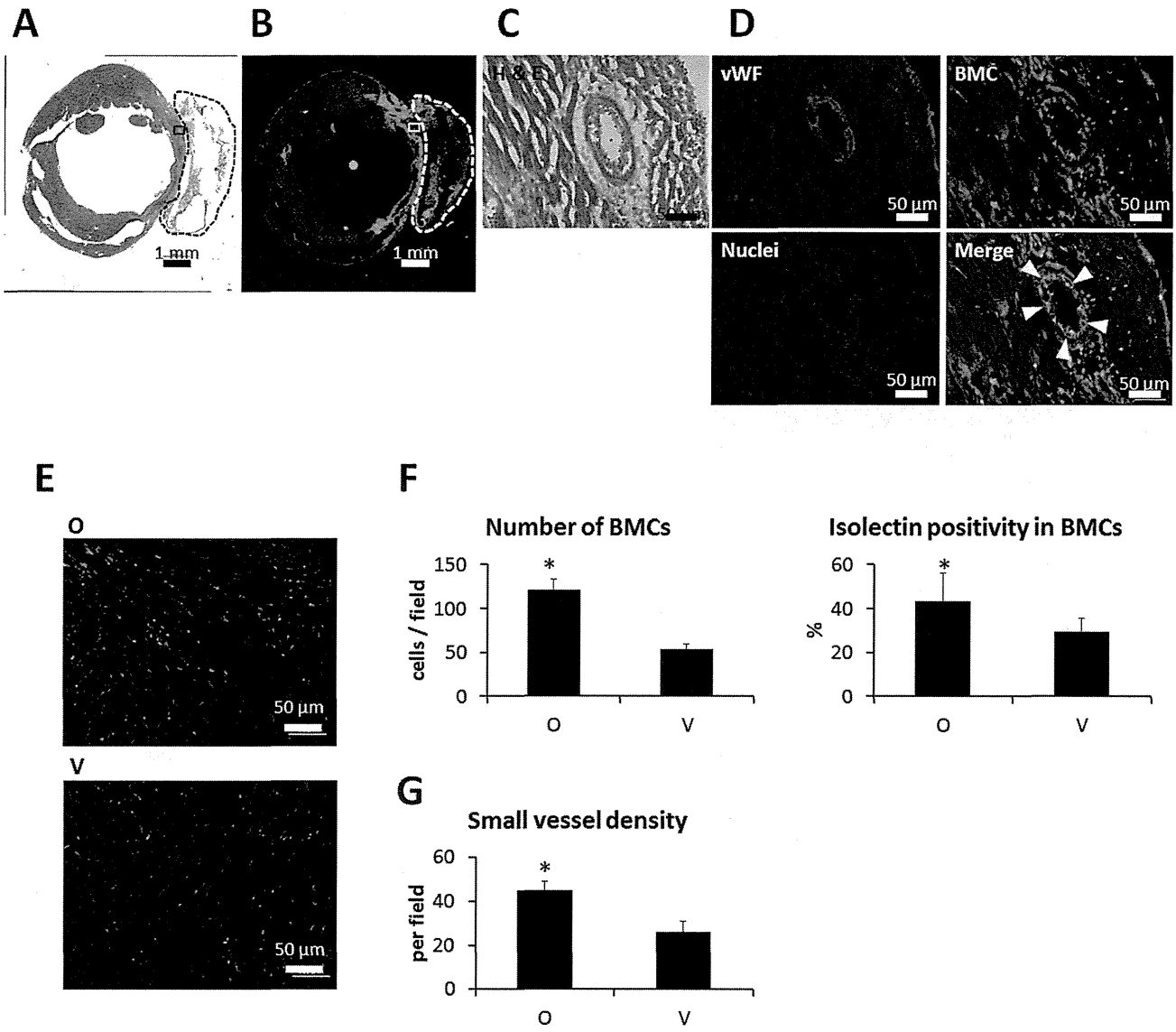

Figure 3. BMCs differentiated into capillary structures in the infarcted area after MI and ONO-1301 treatment. Representative macro image of H and E staining seven days after MI and ONO-1301 treatment. The transplanted sheet is enclosed by a dashed line. A) Serial section of A. The BMCs displayed GFP. B) High-magnification image of the boxed region in A. C) Serial section of C. Arrowheads indicate vWF-expressing BMCs. Red indicates vWF; green, BMCs; and blue, nuclei. D) Representative images of isolectin-stained BMCs seven days after MI and ONO-1301 treatment. E) BMC accumulation and percentages of isolectin-positive BMCs. The number of BMCs that accumulated in the infarcted myocardium was greater in the ONO-1301-treated (O) group than in the vehicle (V) group. The percentage of isolectin-positive BMCs was also greater in the O group than in the V group. *$P<0.05$ vs. V group. F) Small vessel density. Small vessels were detected by CD31 immunostaining. The density of small vessels in the O group was greater than in the V group. *P<0.05 vs. V group.
doi:10.1371/journal.pone.0069302.g003

It is difficult to understand the whole mechanism underlying the functional improvements induced by ONO-1301. It was already reported that ONO-1301 enhances the expression of angiogenic factors HGF and VEGF, leading to angiogenesis and the suppression of fibrosis progression [7,8,9]. In this study, we discovered an alternative mechanism for ONO-1301's therapeutic efficacy in the acute MI mouse, in which the upregulation of SDF-1 promotes BMC accumulation. Stem-cell recruitment and homing are regulated by the interplay of cytokines, chemokines, and proteases. In particular, the SDF-1/CXCR4 axis is central for the mobilization of stem cells from the bone marrow and their homing to ischemic tissues [12]. In the case of ischemic insult, SDF-1 is released by the injured tissue and stimulates the mobilization of progenitor cells from the bone marrow [1,13]. Furthermore, prostaglandins have been reported to facilitate BMC mobilization via upregulation of CXCR4 expression [14,15]. In our experimental setting, ONO-1301 was detected from peripheral blood samples 3 weeks after treatment (Fig. S4 in File S1), suggesting that ONO-1301 may similarly act on the bone marrow to promote the BMC mobilization. Thus, BMC recruitment in the injured myocardium may be enhanced by the upregulation of SDF-1 in cardiac fibroblasts and by the direct upregulation of CXCR4 in BMCs located in the bone marrow. In addition, recent reports show the possibility of endogenous regeneration in the injured heart, including proliferation of postnatal cardiomyocytes and cardiac stem cells [16,17,18,19]. While we were unable to

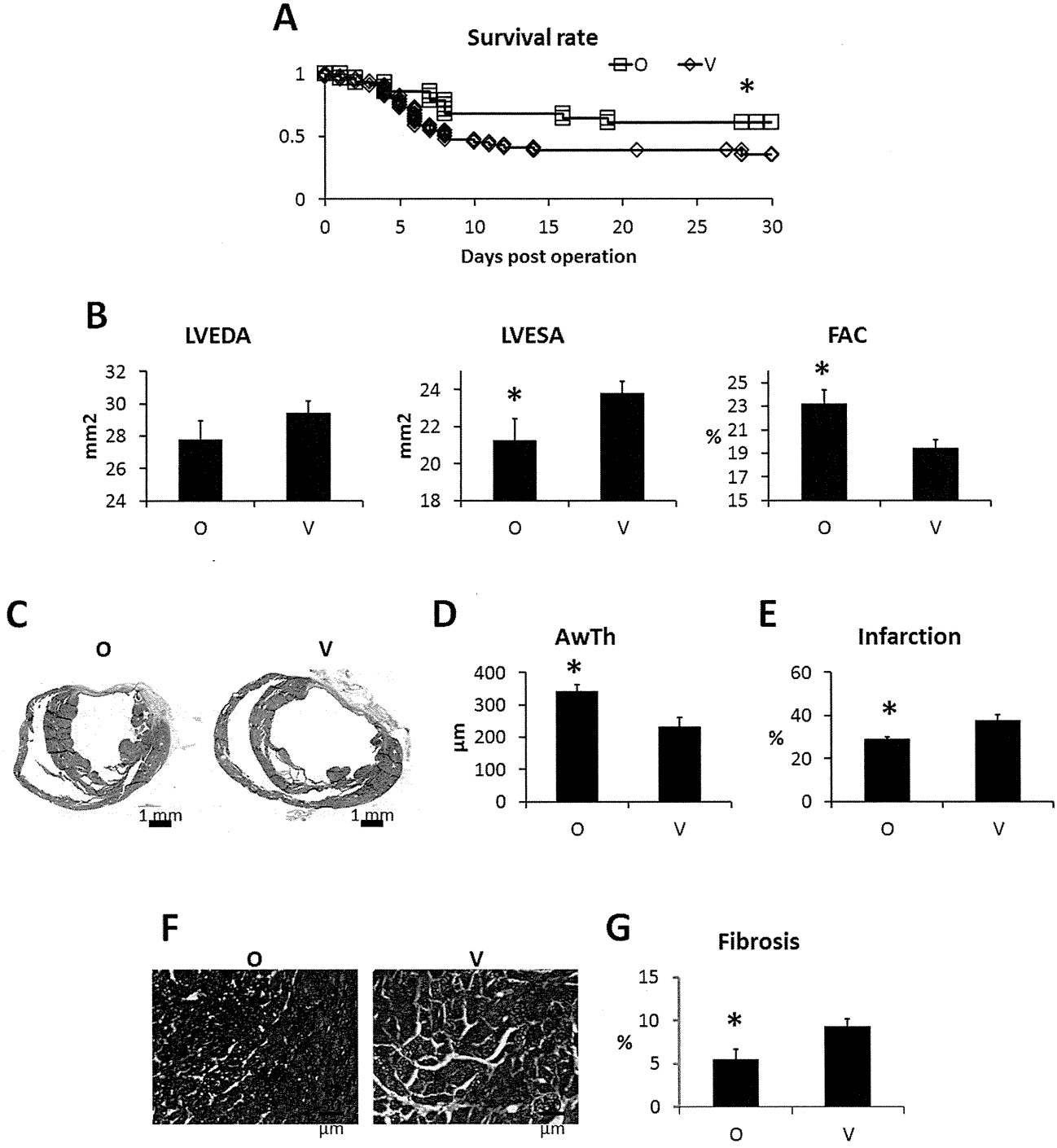

Figure 4. ONO-1301 treatment improved the cardiac performance and survival rate after MI. Survival rates after treatment. The ONO-1301-treated (O) group (n = 33) showed significantly better survival than the vehicle (V) group (n = 48). *$P<0.05$ vs. V group. A) Evaluation of cardiac performance 4 weeks after treatment. In the O group, the LVESA was smaller, and the FAC was significantly higher compared to the V group (O group, n = 22; V group, n = 20; *$P<0.05$ vs. V group). B) Representative macro images from each group. C) Quantification of anterior wall thickness. Anterior wall thickness was significantly thicker in the O group (n = 6) compared to the V group (n = 4). *$P<0.05$ vs. V group. D) Quantification of percent infarction. Infarction was significantly smaller in the O group (n = 6) compared to the V group (n = 4). *$P<0.05$ vs. V group. E) Representative Masson trichrome staining images at the border zone. F) Quantification of fibrosis. Fibrosis at the border zone was significantly smaller in the O group (n = 6) compared to the V group (n = 4). *$P<0.05$ vs. V group.
doi:10.1371/journal.pone.0069302.g004

detect newly-generated cardiomyocytes derived from BMCs in this study, it would be interesting to evaluate the possibility of cardiomyogenesis involving other cell types.

We observed massive BMC accumulation 7 days after MI, including in the infarcted ventricular wall, where they provided structural support in place of the necrotic cardiomyocytes. The